

Feasibility of body electrical loss analysis in detection of abdominal visceral fat

Kim Blomqvist



Feasibility of body electrical loss analysis in detection of abdominal visceral fat

Kim Blomqvist

A doctoral dissertation completed for the degree of Doctor of Science (Technology) to be defended, with the permission of the Aalto University School of Electrical Engineering, at a public examination held at the lecture hall AS1 of the school on 18 January 2019 at 12.

Aalto University
School of Electrical Engineering
Department of Electrical Engineering and Automation
Applied Electronics

Supervising professor

Prof. Ilkka Laakso, Aalto University, Finland

Thesis advisor

Prof. (Emeritus) Raimo Sepponen, Aalto University, Finland

Preliminary examiners

Prof. Ville Kolehmainen, University of Eastern Finland

Prof. Franco Simini, Universidad de la República, Uruguay

Opponent

Dr. Jari Viik, Tampere University of Technology, Finland

Aalto University publication series

DOCTORAL DISSERTATIONS 252/2018

© 2018 Kim Blomqvist

ISBN 978-952-60-8359-9 (printed)

ISBN 978-952-60-8360-5 (pdf)

ISSN 1799-4934 (printed)

ISSN 1799-4942 (pdf)

<http://urn.fi/URN:ISBN:978-952-60-8360-5>

Unigrafia Oy

Helsinki 2018

Finland



Author

Kim Blomqvist

Name of the doctoral dissertation

Feasibility of body electrical loss analysis in detection of abdominal visceral fat

Publisher School of Electrical Engineering

Unit Department of Electrical Engineering and Automation

Series Aalto University publication series DOCTORAL DISSERTATIONS 252/2018

Field of research Applied Electronics

Manuscript submitted 12 September 2018

Date of the defence 18 January 2019

Permission to publish granted (date) 22 November 2018

Language English

Monograph

Article dissertation

Essay dissertation

Abstract

Objective: An excessive amount of abdominal visceral fat has found to be linked to metabolic and cardiovascular health much more than the body mass index (BMI). However, a cost-effective and accurate estimation of abdominal visceral fat accumulation in individuals and groups is hard. This work explores the feasibility of a novel bioimpedance-based method, named as body electrical loss analysis (BELA), aimed at estimating abdominal visceral fat that is in good agreement with estimates obtained using magnetic resonance imaging (MRI).

Approach: During the BELA measurement, the subject's abdomen is covered with a radio frequency coil comprising a tunable high-Q LC resonator. No contact electrodes are attached to the subject standing within the coil. The time-varying magnetic field produced by the coil induces so-called eddy currents in the abdomen. The induced currents oppose the applied magnetic field, and from the coil's point of view power is lost, i.e., the coil is loaded. Lean body tissue that is electrically more conductive than fatty tissue loads the coil more. The loading effect is also heavily dependent on the radial distance of the tissue. So instead of just measuring the losses at some resonant frequency, the novel idea was to measure the rate of loss as a function of frequency. This was expected to have a strong relationship with the internal conductivity of the abdomen, i.e., indicating its level of adiposity.

Main results: A promising correlation ($r = 0.86$ with $SEE = 29.7 \text{ cm}^2$) was found between the loss changing rate measured at the height of umbilicus +5 cm and the visceral fat area obtained with MRI in nine subjects recruited from laboratory personnel and acquaintances. However, the results obtained with the improved prototype in a clinical trial (17 males, 21 females, age 20–68 years, BMI 19.6–39.4 kg/m^2 , and waist circumference 78–128 cm) led to considerably weaker correlation, $r = 0.61$ with $SEE = 59.30 \text{ cm}^2$. Instead, BELA was found to correlate strongly with the circumference of abdominal wall muscles estimated from the waist circumference and the abdominal subcutaneous fat layer thickness measured with the abdominal impedance measurement ($r = 0.86\text{--}0.90$). The relationship with the subcutaneous fat area was found to be weak in both studies ($r < 0.5$), as was expected.

Significance: Although the results do not suggest proposing the BELA in its current form for the prediction of abdominal visceral fat, the novelty of the method is considered a help to guide future studies on bioimpedance-based methods. The strong correlation of BELA with the circumference of abdominal wall muscles suggests its potential in other applications of body composition. The difference between the BELA and the widely used bioimpedance analysis (BIA) is that the BELA relies on the measurement of electrical loss only. No statistical gender, age, or anthropometry is used in the BELA.

Keywords body composition, abdominal visceral fat, electrical bioimpedance, BELA, BIA, MRI

ISBN (printed) 978-952-60-8359-9

ISBN (pdf) 978-952-60-8360-5

ISSN (printed) 1799-4934

ISSN (pdf) 1799-4942

Location of publisher Helsinki

Location of printing Helsinki **Year** 2018

Pages 116

urn <http://urn.fi/URN:ISBN:978-952-60-8360-5>

Tekijä

Kim Blomqvist

Väitöskirjan nimi

BELA-menetelmän soveltuvuus sisäelinrasvan havaitsemiseksi

Julkaisija Sähkötekniikan korkeakoulu**Yksikkö** Sähkötekniikan ja automaation laitos**Sarja** Aalto University publication series DOCTORAL DISSERTATIONS 252/2018**Tutkimusala** Sovellettu elektroniikka**Käsikirjoituksen pvm** 12.09.2018**Väitöspäivä** 18.01.2019**Julkaisuluvan myöntämispäivä** 22.11.2018**Kieli** Englanti **Monografia** **Artikkeliväitöskirja** **Esseeväitöskirja****Tiivistelmä**

Tavoite: Viskeraalinen eli sisäelinten ympärille kertyvä rasva lisää huomattavasti enemmän terveysriskejä kuin ihonalainen rasva. Diabetekseen ja sydänsairauksiin liitetyn sisäelinrasvan mittaaminen tarkasti yksinkertaisin menetelmin on kuitenkin haastavaa. Yleisesti käytetty painoindeksi (engl. body mass index, BMI) ei tee eroa rasvan jakautumisesta sisäelinrasvan ja ihonalaisen rasvan välillä. Myös täysin normaalipainoinen henkilö voi olla sisäisesti lihava. Tässä työssä kehitettiin uudenlainen kehonkoostumusmittaus-menetelmä, jonka soveltuvuutta viskeraalisen rasvan mittaamisessa tutkittiin magneettikvantamisen avulla. Menetelmä nimettiin BELA:ksi, mikä tulee englannin kielen sanoista body electrical loss analysis.

Menetelmä: BELA-mittaus perustuu magneettikentässä tapahtuvien häviöiden havainnointiin. Mitattavan henkilön vatsa ympäröidään kelalla, jolloin kelan tuottama muuttuva magneettikenttä kohdistuu vatsaan pystysuunnassa. Mittaus on kontaktiton eikä erillisinä ihoon liimattavia elektrodeja tarvita. Muuttuvan magneettikentän kudoksiin indusoimien pyörrevirtojen aiheuttama häviö havaitaan kelan kuormittamisena. Pehmytkudos johtaa rasvakudosta huomattavasti paremmin sähkövirtaa, joten se kuormittaa kelaa enemmän. Kehon ulkosäteellä sijaitseva pehmytkudos kuormittaa kelaa myös huomattavasti enemmän kuin sisemmällä säteellä oleva. Ideana oli mitata kelan kuormitus taajuuden funktiona. Tällä ajateltiin olevan yhteys vatsan sisäisen johtavuuden kanssa. Toisin sanoen mitä nopeammin kelan kuormitus kasvaa taajuuden funktiona sitä enemmän mitattavalla henkilöllä olisi sisäistä rasvaa.

Tulokset: Ensimmäiset kokeet yhdeksällä koehenkilöllä antoivat korrelaatioksi 0.86 BELA:n ja magneettikvantamisella mitatun viskeraalisen rasvan pinta-alan välille. Regressioanalyyseille laskettu keskivirhe (SEE) oli 29.7 cm². Kolmekymmentäkahdeksan koehenkilöä sisältävässä jatkotutkimuksessa (17 miestä, 21 naista, ikä 20–68 vuotta, BMI 19.6–39.4 kg/m², vyötärönympärys 78–128 cm) korrelaatio BELA:n ja magneettikuvan välillä jäi kuitenkin selvästi heikommaksi ($r = 0.61$, SEE = 59.30 cm²). Sen sijaan BELA:n havaittiin korreloivan voimakkaasti ($r = 0.86$ – 0.90) vatsan seinämän lihaksien muodostaman ympärysmittan kanssa. Korrelaatio ihonalaisen rasvan pinta-alaan oli molemmissa tutkimuksissa odotetusti heikko ($r < 0.5$).

Tuloksien merkitys: Vaikka saatu korrelaatio ei ole riittävä tarkan regressioyhtälön kehittämiseksi BELA-mittauksen ja magneettikvantamisella havaitun viskeraalisen rasvan välille, tutkimuksen uskotaan auttavan uusien bioimpedanssilaitteiden kehittämistä. Idea häviöiden kasvunopeuden mittaamisesta on kehonkoostumusmittauksissa uusi. Voimakas korrelaatio BELA:n ja vatsan seinämän lihaksien muodostaman ympärysmittan kanssa antaa uskoa siihen, että BELA:aa voitaisiin kehittää uuteen suuntaan. Bioimpedanssianalyyysiin (BIA) verrattuna BELA eroaa siinä, että se perustuu vain mitattuun sähköiseen häviöön. Analyysi ei sisällä henkilön sukupuolta, ikää tai antropometrisiä lisämittauksia.

Avainsanat kehonkoostumus, sisäelinrasva, bioimpedanssi, BELA, BIA, MRI**ISBN (painettu)** 978-952-60-8359-9**ISBN (pdf)** 978-952-60-8360-5**ISSN (painettu)** 1799-4934**ISSN (pdf)** 1799-4942**Julkaisupaikka** Helsinki**Painopaikka** Helsinki**Vuosi** 2018**Sivumäärä** 116**urn** <http://urn.fi/URN:ISBN:978-952-60-8360-5>

Acknowledgements

This work has been carried out, for the most part, at the Department of Electrical Engineering and Automation of the Aalto University School of Electrical Engineering and in part at the Digital Health Lab of Nokia Technologies. I would like to express my gratitude to my instructor Prof. Raimo Sepponen. Without Raimo's innovative mindset and dedication to medical technologies this work would not exist. I would also like to express my gratitude to Prof. Ilkka Laakso for supervising the work. Many thanks go also to the pre-examiners of my dissertation, Prof. Ville Kolehmainen and Prof. Franco Simini, for their detailed comments and suggestions. I'm also grateful to Dr. Jari Viik for agreeing to be an opponent for my dissertation.

Furthermore, this work would not have been possible without the help of my research colleagues Adj. Prof. Nina Lundbom, Dr. Jesper Lundbom and Prof. Kirsi Pietiläinen, who enabled the studies with MRI at Meilahti Helsinki University Hospital. I am also grateful to Dr. Jani Kivioja, Dr. Tapio Taipalus and Dr. Jyri Huopaniemi for making it possible to finalize my dissertation at Nokia. Neither would the work have ever been completed without my colleague and friend Dr. Jussi Kuutti, who tirelessly provided all the help needed to get the last bits and pieces of the work together. I have also received help from Prof. Pekka Eskelinen in electrical measurements and Heikki Ruotoistenmäki in coil mechanics. Also, great thanks to all the volunteers who participated in the studies. Thanks should also go to my parents who have always encouraged me to study hard. Finally I wish to thank my spouse Maarit Korkalainen for her support and patience with the work.

This work was partially supported by the Graduate School of Electrical and Communications Engineering of Aalto University, Biocentrum Helsinki, and the Finnish Society of Electronics Engineers EIS (today known as TiES). The support of all institutions is gratefully acknowledged.

Espoo, December 8, 2018

Kim Blomqvist

Acknowledgements

Contents

Acknowledgements	1
Contents	3
List of Publications	5
Author's Contribution	7
Symbols and Abbreviations	9
1. Introduction	13
1.1 Intra-abdominal obesity: Background and motivation for the thesis	13
1.2 Techniques for measuring intra-abdominal fat	15
1.2.1 Medical imaging	15
1.2.2 Anthropometric techniques	18
1.2.3 Electrical bioimpedance	20
1.3 Electrical bioimpedance via magnetic induction	25
1.4 Scope of the thesis	26
2. Materials and Methods	27
2.1 Body electrical loss analysis (BELA)	27
2.1.1 Instrumentation	29
2.2 Study I: Experiments with phantoms	33
2.2.1 BELA measurement	33
2.3 Study II: Feasibility in human subjects	33
2.3.1 BELA measurement	34
2.3.2 Quantification of fat distribution	34
2.3.3 Statistical analysis	34
2.4 Study III: Clinical trial on human participants	34
2.4.1 BELA measurement	35
2.4.2 Bioelectrical impedance analysis	35
2.4.3 Single-frequency abdominal impedance (SAI)	35

Contents

2.4.4	Quantification of fat distribution	36
2.4.5	Statistical analysis	36
3.	Results	39
3.1	Study I: Experiments with phantoms	39
3.2	Study II: Feasibility in human subjects	40
3.3	Study III: Clinical trial on human participants	40
4.	Discussion	45
5.	Conclusion	49
	References	51
	Corrigenda to Publications	59
	Publications	61

List of Publications

This thesis consists of an overview and of the following publications which are referred to in the text by their Roman numerals.

- I** Kim H. Blomqvist and Raimo E. Sepponen. A feasibility study of altered spatial distribution of losses induced by eddy currents in body composition analysis. *BioMedical Engineering Online*, 9:65, doi:10.1186/1475-925X-9-65, November 2010.
- II** Kim H. Blomqvist, Jesper Lundbom, Nina Lundbom, and Raimo E. Sepponen. Body electrical loss analysis (BELA) in the assessment of visceral fat: a demonstration. *BioMedical Engineering Online*, 10:98, doi:10.1186/1475-925X-10-98, November 2011.
- III** Kim H. Blomqvist, Jussi Kuutti, Jesper Lundbom, Kirsi Pietiläinen, Nina Lundbom, and Raimo E. Sepponen. Quantification of visceral adiposity: evaluation of the body electrical loss analysis. *Biomedical Physics & Engineering Express*, vol. 4, no. 2, doi:10.1088/2057-1976/aaa5bc, January 2018.
- IV** Kim H. Blomqvist, Pekka Eskelinen, and Raimo E. Sepponen. Instrumentation amplifier implements second-order active low-pass filter with high gain factor. *Measurement Science and Technology*, vol. 22, no. 5, doi:10.1088/0957-0233/22/5/057002, April 2011.
- V** Kim H. Blomqvist, Raimo E. Sepponen, Nina Lundbom, and Jesper Lundbom. An open-source hardware for electrical bioimpedance measurement. *In Proc. of 2012 13th Biennial Baltic Electronics Conference (BEC2012), Tallinn, Estonia, October 3–5*, pp. 199–202, doi:10.1109/BEC.2012.6376851, December 2012.

List of Publications

Author's Contribution

Publication I: “A feasibility study of altered spatial distribution of losses induced by eddy currents in body composition analysis”

The author designed and built the tested BELA measuring instrument, carried out the measurements, and drafted the manuscript.

Publication II: “Body electrical loss analysis (BELA) in the assessment of visceral fat: a demonstration”

The author took part in the study design, constructed the BELA measurement setup, carried out the BELA measurements, conducted the correlation analysis, and drafted the manuscript.

Publication III: “Quantification of visceral adiposity: evaluation of the body electrical loss analysis”

The author participated in the clinical study design, designed and built the used BELA instrument, carried out the BELA, BIA, SAI and anthropometric body measurements, interpreted the results, and drafted the manuscript.

Publication IV: “Instrumentation amplifier implements second-order active low-pass filter with high gain factor”

The author invented and designed the amplifier, conducted the circuit simulations and measurements, and drafted the manuscript.

Publication V: “An open-source hardware for electrical bioimpedance measurement”

The author designed and built the open-sourced EBI measuring instrument, conducted the measurements to validate the instrument for the use of abdominal bioimpedance, and drafted the manuscript.

Symbols and Abbreviations

B	vector magnetic field	T
<i>C</i>	capacitance	F
<i>C_m</i>	cell membrane capacitance	F
E	vector electric field	V/m
<i>E_a</i>	electrode a	
<i>E_b</i>	electrode b	
<i>E_i</i>	current injection electrode	
<i>E_{int}</i>	internal E field strength	V/m
<i>E_{rms}</i>	root mean square value of E field	V/m
<i>E_v</i>	voltage sensing electrode	
<i>f</i>	frequency	Hz
<i>f₀</i>	resonant frequency	Hz
<i>f_H</i>	higher resonant frequency	Hz
<i>f_L</i>	lower resonant frequency	Hz
<i>h</i>	height	m
<i>I_p</i>	primary current of current transformer	A
<i>j</i>	imaginary unit, $j = \sqrt{-1}$	
<i>L</i>	inductance, or length	H, m
<i>m_{loss}</i>	rate of eddy current loss	V/Hz
<i>N</i>	number of coil windings	
<i>P</i>	power loss	W
<i>Q</i>	quality factor	
<i>R</i>	electrical resistance	Ω
<i>R²</i>	“R squared”; the coefficient of determination	
<i>R₀</i>	tissue DC resistance	Ω
<i>R₅₀</i>	total body resistance at 50 kHz	Ω

Symbols and Abbreviations

R_e	extra-cellular resistance of biological tissue	Ω
R_g	gain resistor	Ω
R_i	intra-cellular resistance of biological tissue	Ω
R_{loss}	ohmic losses	Ω
R_T	terminal resistor of current transformer	Ω
R_∞	tissue AC resistance at infinite frequency	Ω
r	radius, or correlation coefficient	m, –
V_0	excitation, or sensed voltage	V
V_b, V_{bias}	bias voltage	V
V_{in}	input voltage	V
V_{out}	output voltage	V
X	electrical reactance	Ω
X_C	capacitive reactance	Ω
X_L	inductive reactance	Ω
Z	electrical impedance	Ω
ρ	resistivity	$\Omega \cdot \text{m}$
σ	standard deviation	
σ_{eff}	effective electrical conductivity	S/m
σ_H	standard deviation of the mean voltage change across the coil at higher frequency	
σ_L	standard deviation of the mean voltage change across the coil at lower frequency	
ω	angular frequency, $\omega = 2\pi f$	rad/s
A/D	analog-to-digital converter	
BELA	body electrical loss analysis	
BIA	bioimpedance analysis	
BMI	body mass index	
BPF	band-pass filter	
D/A	digital-to-analog converter	
DC	direct current	
EBI	electrical bioimpedance	
ECF	extracellular fluid	
EEOC	The U.S. Equal Employment Opportunity Commission	
EIT	electrical impedance tomography	
EMR	electromagnetic resonance	

FFM	fat-free mass
ICF	intracellular fluid
IDF	International Diabetes Federation
INA	instrumentation amplifier
L1	first lumbar vertebra
L2	second lumbar vertebra
L3	third lumbar vertebra
L4	fourth lumbar vertebra
L5	fifth lumbar vertebra
LOOCV	leave-one-out cross-validation
LPF	low-pass filter
MIT	magnetic induction tomography
MR	magnetic resonance
MRI	magnetic resonance imaging
NIH	National Institutes of Health, a part of the U.S. Department of Health and Human Services
NS	normal saline, a mixture of sodium chloride in water (9.0 g per litre)
OPAMP	operational amplifier
REF	reference
RF	radio frequency
RMS	root mean square
S1	first sacral bone
SAD	sagittal abdominal diameter
SAI	single-frequency abdominal impedance
SEE	standard error of the estimate
SF	subcutaneous fat
SFA	subcutaneous fat area
SFL	subcutaneous fat layer
TBW	total body water
TOBEC	total body electrical conductivity
TOFI	“thin-outside-fat-inside” phenotype
TRIM	tissue resonant impedance monitor
USB	Universal Serial Bus
VF	visceral fat
VFA	visceral fat area
WC	waist circumference

Symbols and Abbreviations

WC_{eff}	BELA effective waist circumference
WHR	waist–hip ratio
WHO	World Health Organization
$^{\circ}\text{C}$	degree Celsius
%BF	percentage of body-fat mass

1. Introduction

1.1 Intra-abdominal obesity: Background and motivation for the thesis

Obesity, the excess of body fat, has increased worldwide. The World Health Organization (WHO) has estimated that in 2016 13% of adults aged 18 years and above were obese [1], i.e., their body mass index (BMI) was 30 or above. Anyone can easily determine their BMI by measuring their weight in kilograms and dividing it by the square of their height in metres (kg/m^2). For comparison, adults who fall into the BMI range of 18.5 to 24.9 are considered to have normal weight, and those with BMI 25 to 29.9 are considered overweight. Furthermore, the BMI metric classifies obesity into three subcategories: I, II and III, where class III ($\text{BMI} \geq 40$) means extreme, or morbid, obesity. A historical review of how these categories have been established is given in [2].

Obesity increases the risk of developing cardiovascular diseases, stroke, diabetes, and some forms of cancer [1, 3]. However, regardless of BMI, obesity-related complications have found to vary significantly between individuals [3–6]. Although obesity is likely to decrease the quality of life in terms of physical state, vitality, relations with others, and psychological state [7, 8], a small part of the obese remain metabolically healthy. Metabolism includes the process by which our body converts what we eat and drink into energy. A disruption in this process leads to metabolic disorder, e.g. diabetes. Metabolic syndrome, in turn, consists of a group of conditions that put us at risk for metabolic disorder. These conditions are, e.g., elevated blood pressure, high blood sugar, excess body fat around the waist, and abnormal cholesterol or triglyceride levels. It has been estimated that approximately 10% of obese adults in the United States (1999–2004) were metabolically healthy, i.e. had less than two metabolic abnormalities [9]. Simultaneously, 8% of people with normal weight were considered metabolically unhealthy (≥ 2 metabolic abnormalities). Furthermore, a study from 2016 reported that almost 75 million U.S. adults were misclassified by BMI either as metabolically unhealthy or metabolically healthy [10]. Thus there is

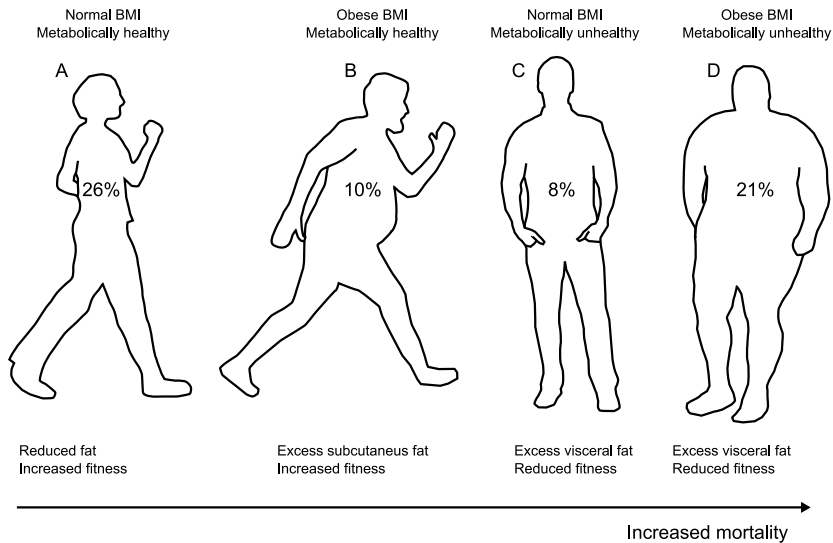


Figure 1.1. An excessive amount of visceral fat tends to be linked to the metabolic syndrome. Among the United States adults (1999–2004), approximately 10% were obese by their BMI but yet metabolically healthy. Simultaneously 8% were normal weight but metabolically unhealthy. In contrast, 26% of adults with normal BMI were metabolically healthy and 21% with obese BMI were metabolically unhealthy [9]. The Figure is adapted by the author from [4].

an urgent need for a better predictor of metabolic syndrome [4]. Better metrics are also increasingly important as, e.g., the U.S. Equal Employment Opportunity Commission (EEOC) have set rules allowing employers to offer incentives based on whether the employee achieves certain health outcomes in the workplace's wellness program [11]. Thus a concern has been raised that employers may be tempted to charge employees with higher BMI more for their health insurance although they can be healthier than employees with normal BMI [10].

As shown in Figure 1.1, an excessive amount of intra-abdominal fat, also known as abdominal visceral fat or just visceral fat (VF), has found to be linked to metabolic and cardiovascular health much more than BMI [12, 13]. In contrast to abdominal subcutaneous fat (SF) that is located directly under the skin, visceral fat is stored within the abdominal cavity. Visceral fat tends to wrap around internal organs such as the stomach, liver and intestines, and it is suggested to be biologically active. Because of its location, the substances released by visceral fat may enter the portal vein and travel to the liver, where they can influence the production of blood lipids in a disadvantageous way. The portal vein is located in the right upper quadrant of the abdomen. All the blood that leaves the spleen, stomach, small and large intestine, gallbladder and pancreas is collected by the portal vein and supplied to the liver. That is approximately 75–80% of the blood entering the liver [14]. Thus visceral fat is considered more harmful than subcutaneous fat. An appropriate amount of subcutaneous fat without the excess accumulation of visceral fat may even have positive

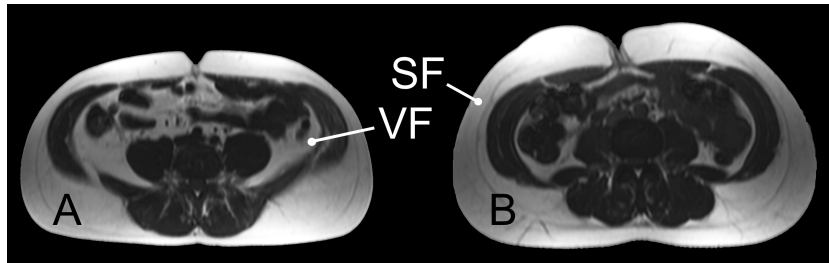


Figure 1.2. Abdominal fat areas, appearing in white, obtained with magnetic resonance imaging. Subject A with normal BMI (24.9) had VF with a surface area of 112.8 cm^2 , whereas B with overweight BMI (29.3) had only 36.2 cm^2 .

biologically important roles, such as elimination of toxic lipids and maintenance of hormonal regulation, thereby improving metabolic and cardiovascular health in some obese people [15–18].

In summary, the body-fat distribution between the subcutaneous and visceral fat depots plays an important role in metabolic health. Although low total body-fat level is generally associated with a low level of abdominal visceral fat, a considerable variation exists between individuals. You may have visceral fat but yet not be obese, or you may be obese but with an excess amount of subcutaneous fat only. This has been further demonstrated in Figure 1.2 that shows a cross-sectional axial image of the abdominal fat areas obtained by magnetic resonance imaging (MRI). The two volunteers compared in Figure 1.2 took part in the research study reported in [III]. Subject A with normal weight BMI had over three times more visceral fat than subject B with higher BMI. An additional example would be a study from 2011 based on a UK-based cohort, where 14% of men and 12% of women with BMI 18.5–25 were considered “thin outside but fat inside” (TOFI), as they had a disproportionate amount of visceral fat stored within their abdomen despite the desirable BMI [19].

Medical imaging such as MRI is a very accurate method to measure visceral fat but also very expensive. Instead, it would be beneficial if visceral fat could be measured with a simple method without the need of medical personnel to perform the measurement and interpret the result. This is the problem to which this work contributes to.

1.2 Techniques for measuring intra-abdominal fat

1.2.1 Medical imaging

Computed tomography (CT) and MRI are the current gold standard techniques for the quantitative assessment of intra-abdominal fat, providing the most accurate, specific and comprehensive data [20]. There is also a good agreement

between the methods to measure both the visceral and subcutaneous parts of fat [21]. However, due to high operating cost and limited availability of such expensive equipment, neither method is suitable for use in periodic health check-ups. A drawback of the CT is that it also exposes subjects to ionizing radiation. Otherwise, it is considered less expensive and is better available than MRI. Also, subjects who have metal fragments or devices, such as a pacemaker, in their body can use CT because no magnetic field is involved. Furthermore, claustrophobic subjects may find CT more comfortable, as the scanners are typically shorter and less noisy than MRI. A more convenient MRI would be an open low-field MRI [22], but its availability tends to be even worse. Lastly, both CT and MRI are equally uncomfortable in that they require the subject to suspend breathing during image acquisition. To get an idea how the installations look like, the MRI scanner used in [III] is shown in Figure 1.3.

The information on accumulated visceral fat obtained with either CT or MRI is often determined from single- or multi-slice images centred at the umbilicus or at the level of the L2–L3 or the L4–L5 lumbar intervertebral disc [23, 24], as visualized in Figure 1.4. The slice thickness varies in the literature from 0.5 cm to 1 cm [24]. Both single- and multi-slice protocols are appropriate to compare differences among the subjects, but the multi-slice protocol is thought to be more suitable for longitudinal studies to track changes in the amount of fat [24]. After the scan, a radiologist examines the images for the surface areas of visceral and subcutaneous fat, denoted as VFA and SFA, respectively. This usually happens either manually or in a semi-automatic manner. In addition, also fat volumes and masses can be derived from the images.

Japanese with VFA $\geq 100 \text{ cm}^2$ at the umbilical level are considered visceraally obese [25, p. 1977]. At this threshold, the prevalence of metabolic abnormalities



Figure 1.3. A 1.5-Tesla MRI scanner with a 70 cm wide bore photographed from the door of the radio frequency (RF) shielded MRI room. This particular scanner, located at Meilahti Helsinki University Hospital, was used in [III].

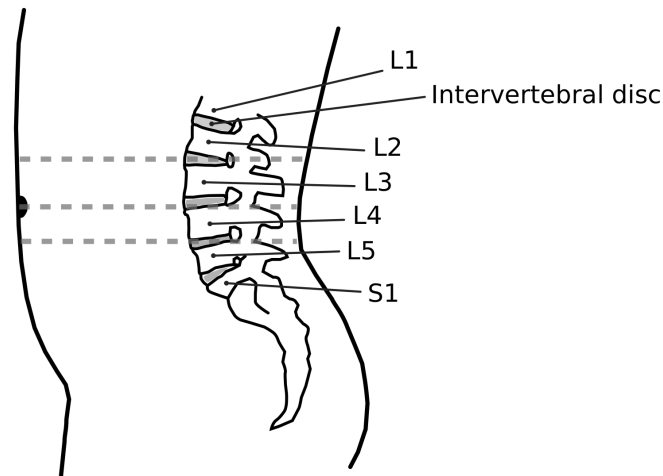


Figure 1.4. The lateral view of lumbar spine. The dotted red lines indicate the CT and MRI imaging sites commonly used to differentiate and quantify abdominal fat compartments. From top to bottom the shown measurement sites are L2–L3, umbilicus, and L4–L5.

has been found to be increased in Japanese men and women equally [26, 27]. The same 100-cm^2 threshold has been also used in French-Canadian subjects to identify the optimal cut-off point for the waist circumference to estimate VFA obtained with MRI at the level of L4–L5 [28]. However, the amount of VFA in one subject may substantially vary at different measurement sites/levels [29]. Thus caution should be taken when comparing the measured VFAs between studies.

In addition to CT and MRI, dual-energy X-ray absorptiometry (DXA, formerly DEXA) [30, 31] and ultrasound [32] can also be used for body composition assessment. DXA is typically used to diagnose and follow osteoporosis [33], but since the measurement of abdominal visceral fat is a rather hot topic, manufacturers such as GE Medical Systems Lunar (a subsidiary of GE Healthcare Ltd., Madison, WI, USA) and Hologic Inc. (Bedford, MA, USA) have steered the development of DXA towards body composition assessment [31]. The key benefits of DXA and ultrasound are cost-effectiveness and a smaller need for space. A study from 2016 showed that DXA is both accurate and valid among a large, multiethnic cohort within a wide range of body fatness [34]. The relationship between the MRI was found to be $R^2 = 0.82$ for females and $R^2 = 0.86$ for males [34]. A more recent study, however, concluded that because the precision of DXA decreases with the increasing BMI, caution should be used with estimates obtained with DXA in obese adults [35]. Furthermore, DXA still exposes subjects to ionizing radiation, even though the radiation dose is very small. Ultrasound, in turn, does not expose subjects to ionizing radiation. It was first used to assess VFA in 1990. The correlation between the intra-abdominal thickness obtained with ultrasound and the VFA obtained with CT was found to be $r = 0.669$ [36].

Twenty-one years later, a strong relationship ($r = 0.85$) was reached between CT and ultrasound measures of visceral fat [37]. However, the results obtained with ultrasound are highly dependent on operator proficiency, thereby reducing the reproducibility of the method [20, 32], i.e., the degree of agreement between the results of experiments conducted by different individuals at different locations with different instruments. Similarly, regarding DXA, a concern has been raised about inter-device differences in assessing VFA between two dominant DXA manufacturers, GE Healthcare and Hologic [38]. Furthermore, despite the lower costs, neither DXA nor ultrasound have yet been used to measure visceral fat, e.g., in occupational health checks.

1.2.2 Anthropometric techniques

Anthropometry is the study of human body measurements including shape, dimensions, proportions and mass, as well as strength and mobility. The word anthropometry is derived from the Greek ‘anthros’, meaning man, and ‘metron’, meaning measure. BMI is an anthropometric body measure, but not to assess central obesity. To assess central obesity, waist circumference (WC) is arguably the most widely used with a fairly good correlation to VFA obtained with either CT or MRI. The mean correlation \pm standard deviation across a few papers is $r = 0.74 \pm 0.08$ for women and 0.79 ± 0.04 for men [28, 39–41]. Figure 1.5 shows the waist circumference measurement sites recommended by the WHO and the U.S. National Institutes of Health (NIH). According to the WHO guidelines, the waist circumference is measured midway between the lowest rib and the iliac crest, whereas the NIH recommends measuring the waist circumference immediately above the iliac crest [42]. In the assessment of VFA, the choice of the measurement site has an effect mainly in women. In men and underage children the different measurement sites tend to yield similar results [41]. For

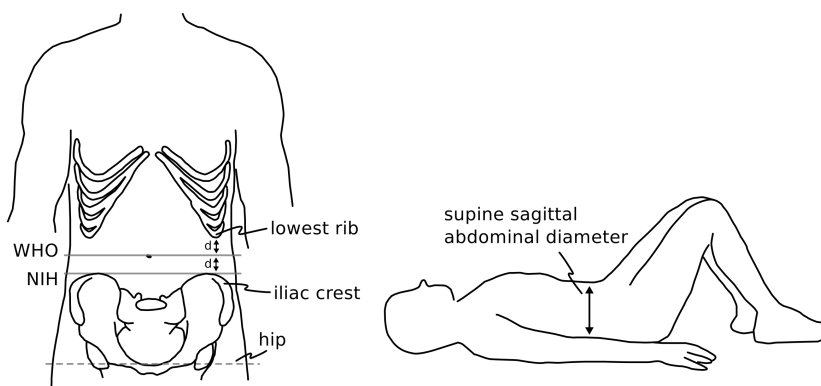


Figure 1.5. Waist circumference measurement sites (solid lines) as recommended by WHO and NIH. The hip circumference is measured at the largest circumference of the buttocks (dashed line). The sagittal abdominal diameter, i.e., abdominal height, is commonly measured in the supine position.

accurate measurements, the posture, respiratory phase, and meal time are also worth taken into consideration [43]. A three-dimensional body scanner using white light can automate the measurement of waist circumference with improved reliability [44, 45].

The waist–hip ratio (WHR) and sagittal abdominal diameter (SAD) are two other anthropometric body measures to estimate central obesity. The WHR is measured as a ratio of the waist circumference to hip circumference, where the hip circumference is measured at the largest circumference of the buttocks (see Figure 1.5). The SAD, in turn, is equal to ‘abdominal height’ usually measured with the subject in a supine position. A fairly strong correlations (women $r = 0.82 \pm 0.08$; men $r = 0.81 \pm 0.01$) have been reported between the SAD and the VFA obtained with CT [39, 40]. Similarly, the correlations found between the WHR and VFA are $r = 0.53 \pm 0.12$ in women and 0.76 ± 0.04 in men [28, 39, 40].

Despite fairly strong correlation to abdominal visceral fat, the simple body measures have their limitations. The measurements cannot really differentiate between the abdominal subcutaneous fat and abdominal visceral fat. Waist circumference is actually better correlated ($r \geq 0.85$) with abdominal subcutaneous fat than with abdominal visceral fat [41], and thus obviously not sensitive to subjects with TOFI phenotype. Furthermore, neither waist circumference nor waist–hip ratio provide a proper response to the changes in visceral fat depots [41, 47]. Moreover, anthropometric measures are affected by ethnic differences [48], and commonly also sex and age-adjusted. Instead of using anthropometry to estimate the abdominal visceral fat, it is more often used to assess the risk of metabolic complications. This is also what is recommended by a report of a WHO expert consultation: “the basis for effective use of waist circumference and waist–hip ratio cut-off points in clinical and public health should relate to health outcomes rather than to associations with intra-abdominal fat, because risk prediction is more straightforward if based on health outcomes” [46, p. 24]. The WHO cut-off points referred to in the recommendation are given in Table 1.1. In comparison, the cut-offs for waist circumference provided by the International Diabetes Federation (IDF) are 94 cm for European men and 80 cm for European women. For South Asians, Chinese, and Japanese the respective cut-off points by IDF are 90 cm for men and 80 cm for women [46, p. 28].

Table 1.1. World Health Organization cut-off points of WC and WHR to predict individual metabolic risk in Caucasians. The Table is adapted by the author from [46, p. 27].

Indicator	Cut-off points		Risk of metabolic complications
	Men	Women	
WC	> 94 cm	> 80 cm	Increased
WC	> 102 cm	> 88 cm	Substantially increased
WHR	≥ 0.90	≥ 0.85	Substantially increased

1.2.3 Electrical bioimpedance

Electrical bioimpedance (EBI) methods are based on measuring electrical voltage across the biological tissue, or body region, while a known alternating current is injected through the tissue/region. From the measured voltage and the known current, the so-called bioimpedance, i.e., the tissue's ability to impede the electrical current, is calculated as

$$Z(\omega) = \frac{V(\omega)}{I(\omega)}, \quad (1.1)$$

where Z is the bioimpedance, V is the measured voltage, I is the applied current, and $\omega = 2\pi f$ is the angular frequency of the current. The obtained impedance Z is a complex quantity of the form

$$Z = R - jX_C = R + \frac{1}{j\omega C}, \quad (1.2)$$

where $j = \sqrt{-1}$ is the imaginary unit, R is the electrical resistance, X_C is the capacitive reactance, and C is capacitance. The resistance R in Equation 1.2 is related to tissue electrical resistivity, ρ , which for a uniform piece of tissue or material is defined as

$$\rho = R \frac{A}{L}, \quad (1.3)$$

where L is the length and A the cross-sectional area of the piece of tissue/material. Typical tissue resistivities obtained in whole-body impedance studies are shown in Table 1.2. The difference between the fat and muscle tissue is about tenfold.

The frequency-dependent reactive component X_C in Equation 1.2 is caused by the cell membrane. Considering the biological tissue as a suspension of spherical cells [49], the current flowing through the tissue follows different paths at different frequencies, as shown in Figure 1.6a. Low-frequency currents, including the direct current (DC), do not pass through the cell, and thus flow mainly in the extracellular fluid (ECF) of the tissue. High-frequency currents,

Table 1.2. Tissue resistivities at 37 °C. The Table is adapted by the author from [49].

Tissue	Resistivity ($\Omega \cdot \text{m}$)	
	10 kHz	1 MHz
Bone	100	50
Fat	15–50	15–50
Blood	1.5	1.5
Muscle (perpendicular to fibers)	10	1.3–1.7
Muscle (parallel to fibers)	2	0.6–0.8

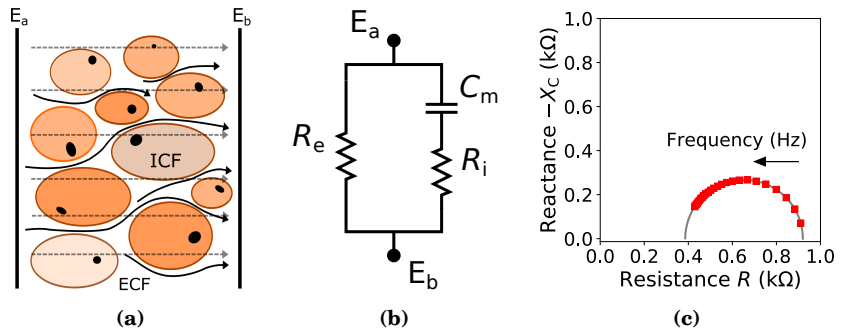


Figure 1.6. (a) Low- and high-frequency current paths (solid and dotted lines, respectively) in biological tissue from electrodes E_a to E_b . (b) The biological tissue equivalent circuit model. (c) The Cole-Cole plot showing the measured impedance in 4-kHz steps from 4 kHz to 100 kHz. The fitted line shows the frequency response from zero to infinity.

instead, penetrate the cell membrane, and thus also “probe” the intracellular fluid (ICF) of the tissue. Figure 1.6b further shows an equivalent electrical circuit of the tissue. The conductive parts of the intra- and extracellular fluid volumes are denoted as R_i and R_e , respectively, of which R_i is isolated by a capacitive cell membrane C_m . Substituting $R_i = 665 \Omega$, $R_e = 920 \Omega$ and $C_m = 3.4 \text{ nF}$ [50] in the model, yields the frequency response shown in Figure 1.6c. The red dots show the impedance values in 4-kHz steps from 4 kHz to 100 kHz. The points where the curve crosses the x-axis show the tissue bulk-resistance at DC and infinite frequency, $R_0 = 920 \Omega$ and $R_\infty \approx 386 \Omega$, respectively. These resistance values can be used to predict the proportions of ECF and ECF + ICF [51]. E.g., ECF and ICF together allows estimating total body water (TBW), which under normal hydration conditions is roughly 73% of the fat-free body mass (FFM) [51].

Bioimpedance analysis

Bioimpedance analysis (BIA) is a widely used method to estimate whole body compartments [51]. Body-fat scales, e.g., by OMRON Healthcare (a subsidiary of OMRON Co., Ltd., Kyoto, Japan) are widely available for purchase by lay people from any hypermarket. In occupational health checks the measurement is often known as “InBody measurement” in accordance with the device name provided by InBody Corporation, Seoul, Korea. Originally the BIA measurement has been performed in a supine position from wrist to ankle, but with the scales becoming more common the measurement is nowadays taken in standing position from ankle to sole as illustrated in Figure 1.7. Usually the four-electrode measurement, i.e., the tetra-polar impedance technique, is used. This means separate electrodes for the current injection and voltage sensing. This way the effects of the electrode-to-skin impedance are minimized [49], provided that both the output impedance of the current source and the input impedance of the voltage sensing differential amplifier are large as compared with the sum of the electrode and tissue impedances [52, p. 12]. Depending on the frequencies used,

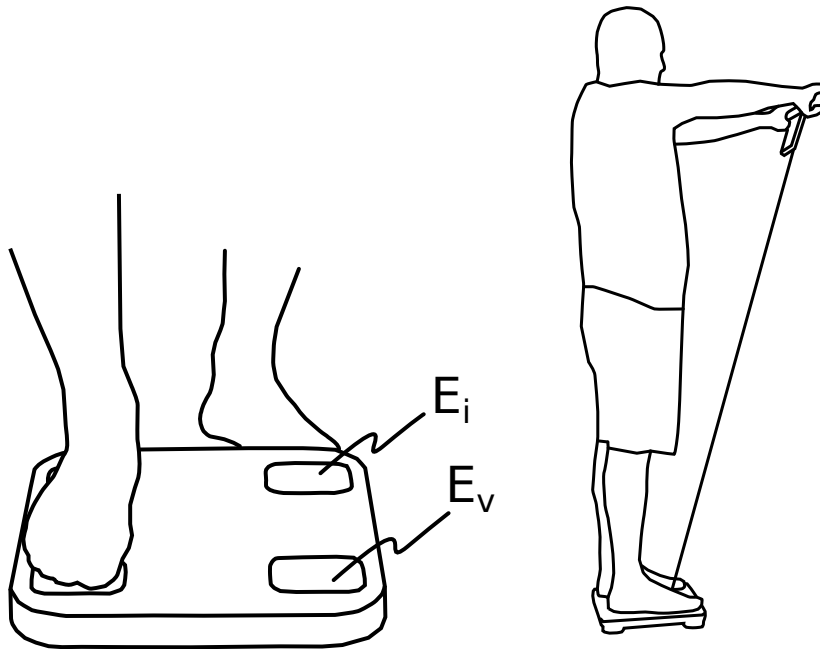


Figure 1.7. An illustration of the use of a commercially available body-fat scale with hand grip. Electrode E_i is for the current injection and E_v for the voltage sensing. Rather than measuring the whole-body bioimpedance from wrist to ankle, the measurement is performed from palm to sole.

the method is either called single-frequency BIA (SF-BIA) or multiple-frequency BIA (MF-BIA) [49]. SF-BIA is usually performed at 50 kHz, whereas MF-BIA utilizes at least two frequencies where the lower frequency is generally less than 20 kHz and the higher frequency more than 50 kHz [51]. The currents injected typically ranges from 100 μA to 800 μA in amplitude [52, p. 228], but as low as 1–10 μA have also been used [49].

The BIA parameter Ht^2/R_{50} , i.e., body height squared divided by the resistance obtained by BIA at 50 kHz, is known to have a strong linear relationship with fat-free mass [49, 53]. The parameter has its analogy in cylindrical body volume, $\text{Vol} = \rho L^2/R$ [54, p. 9]. However, despite the favorable relationship to fat-free mass, many equations predicting the fat-free mass also include sex, age and additional anthropometry, as they have been found to be significant predictors in heterogeneous groups of individuals. For Europeans 16 years old or older, the fat-free mass can be obtained, e.g., with

$$\begin{aligned} \text{FFM} = & 0.340 \times 10^4 Ht^2/R_{50} + 15.34 Ht + 0.273 Wt + 4.56 \text{ Sex} \\ & - 0.127 \text{ Age} - 12.44, \end{aligned} \quad (1.4)$$

where R_{50} is the total body resistance at 50 kHz, Ht is body height in metres, Wt is body weight in kg, Age is age in years, and Sex is either 1 or 0 (male or

female, respectively) [55]. Equation 1.4 is just one of many prediction equations developed for estimating fat-free mass. With a few exceptions, the correlation between the fat-free mass and the prediction equations recommended in research reports have been over 0.9 for R^2 with the standard error of the estimate (SEE) being less than 3 kg [53]. In studies predicting the percentage of body-fat mass (%BF), the typical values for R^2 have ranged from 0.60 to 0.96, with SEEs of 3.3–5.0% [53].

As BIA has proven to be beneficial in estimating fat-free mass, it has been tempting to apply BIA also for abdominal visceral fat. A moderately strong correlation ($r = 0.759$) between the VFA obtained with CT and VFA estimated by InBody 720 body composition analyzer has been found in a study of 53, presumably Japanese, patients with gastric cancer [56]. In a study of Korean-based cohort consisting of 1006 adults with BMI 17–46 kg/m², the correlation between the VFA estimated by InBody 720 and the VFA obtained with CT, however, remained modest ($r = 0.605$) [57]. A similar correlation ($r = 0.64$) was also found in a study of 102, presumably Koreans, healthy individuals with BMI 13–35 kg/m² [58]. For the X-scan body composition analyzer (Jawon Medical Co., Ltd., Daejeon, South Korea), an InBody-like device, the correlation between the VFA estimated by BIA and the VFA obtained with CT was found to be strong ($r = 0.870$) when studying 104, presumably Turkish, healthy adults with BMI 18.3–52.8 kg/m² [59]. Furthermore, in a study of nineteen Caucasian obese adults (mean BMI 34.6 kg/m²), the correlation between the VFA obtained with MRI and the VF level estimated by the body-fat scale (BF-530; OMRON Healthcare) was found to be $r = 0.40$, and it rose to $r = 0.78$ after a 5-month weight-loss intervention [60]. In comparison to ‘bathroom-BIA’, such as OMRON BF-530, InBody provides segmental body analysis [61]. InBody also claims not to use any statistical variables, such as sex, age, or body type in its analysis [61]. However, this probably applies to estimating fat-free mass only, whose correlation to DXA has been reported in [62]. Moreover, although theoretically preferable, segmental BIA is considered not to show much advantage over conventional whole-body wrist-to-ankle approaches [63].

Abdominal BIA

Unlike whole-body BIA, abdominal BIA, or local BIA, measures the impedance in the abdominal region. Figure 1.8 shows the electrode placement for the abdominal BIA especially developed for the measurement of abdominal visceral fat [64]. For this particular BIA method, the correlation of $r = 0.88$ was found between the VFA determined by CT and the VFA estimated by

$$\text{VFA} = a_0 + a'_1 V_0 \text{Wc}^3, \quad (1.5)$$

where a_0 and a'_1 are constants, Wc is the waist circumference at the umbilical level, and V_0 is the voltage measured at the flank, as shown in Figure 1.8. In another study using a slightly different electrode position [65], a correlation of

$r = 0.920$ was found between the VFA obtained with CT and the VFA predicted by

$$\begin{aligned} \text{VFA} = & 2.26 \text{EBI}_{100} + 3.74 \text{SAD} + 132.77 \text{WHR} + 0.85 \text{Wt} + 0.93 \text{Age} \\ & - 17.61 \text{Sex} - 214.54, \end{aligned} \quad (1.6)$$

where EBI is the electrical bioimpedance measured across the abdomen at 100 kHz in the supine position, as illustrated in Figure 1.9, SAD is the sagittal abdominal diameter, WHR is the waist–hip ratio, Wt is body weight, Age is age in years, and Sex is 1 for men and 2 for women. For commercially available abdominal BIA, the correlation of $r = 0.89$ has been found for OMRON DUALSCAN HDS-2000 [58] and $r = 0.64\text{--}0.79$ for ViScan AB-140 (Tanita Corporation, Tokyo, Japan) [66–69].

Electrical impedance tomography

Adding more electrodes around the abdomen enables the so-called electrical impedance tomography (EIT), in which the electrical impedance values measured from the surface electrodes are used to form a tomographic image. EIT

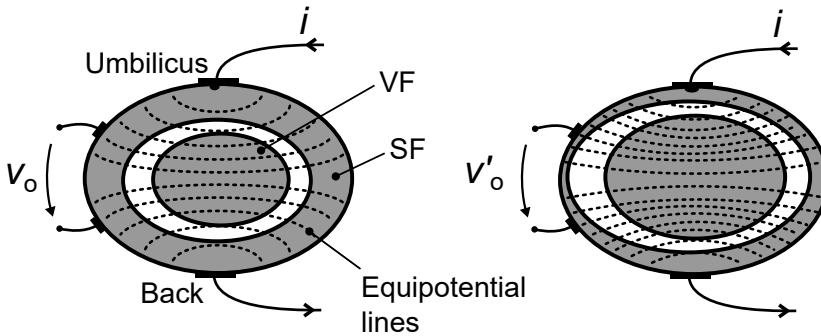


Figure 1.8. Abdominal BIA measurement as conducted in [64]. The alternating current i was injected across the abdomen between the umbilicus and the back. The voltage V_0 measured at the flank was thought to become larger with the accumulation of visceral fat (i.e., $V'_0 > V_0$). The Figure is adapted by the author from [64].

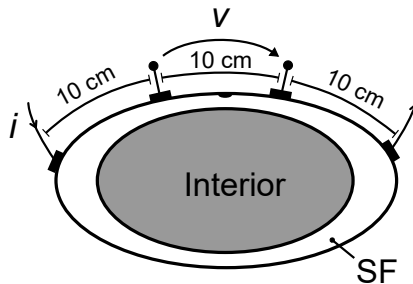


Figure 1.9. Electrode position of abdominal BIA as conducted in [65]. The Figure is adapted by the author from [65].

has been found to be particularly useful for monitoring of lung function [52, pp. 36–39], but for the assessment of abdominal visceral fat there are only little published research. Primarily one research group has been trying to measure visceral fat with EIT [70, 71]. Based on the reconstructed images, EIT seems to be capable of revealing the abdominal subcutaneous fat and muscles, but the fat around the internal organs is not visible in the images. Probably because of this, the latest research in 2018 has concentrated more on the estimation of the boundary of the abdominal subcutaneous fat than the measurement of visceral fat [72].

1.3 Electrical bioimpedance via magnetic induction

Electrical bioimpedance can be also measured without contact electrodes through magnetic induction, i.e., by measuring a change in the magnetic field when “loaded” by the body. Total body electrical conductivity (TOBEC), a human body composition analyzer introduced in the early 1980s, is an example of such a method [73, 74]. The method operated on the principle that the impedance of the coil, driven by a 5-MHz oscillating RF current, was changed when the subject was inserted into a solenoidal coil long enough to cover the whole body. The change in the coil’s impedance was then used to estimate body water content and fat-free mass. Paediatric TOBEC, especially designed to be used for neonates and small children, tended to provide accurate data, but in general the use of the TOBEC method suffered from limited acceptance due to high cost, cumbersome equipment, and patient logistics [75, p. 79]. Additionally, the method had issues with uncontrolled capacitive couplings [75, p. 96, 100]. Although having limited success in human body measurements, today TOBEC is still used in body-composition analysis of small animals. The latest use in human body composition (paediatric TOBEC) seems to be from 2009 [76].

Another TOBEC-like instrument is tissue resonant impedance monitor (TRIM) [77]. The idea here was to measure the frequency shift in the impedance minimum of a helical coil around 2 MHz as the test subject was placed into the coil. In the middle of the 1990s, a larger version of TRIM was introduced and named electromagnetic resonance (EMR) [78]. The observations made with the EMR coil by using saline phantoms suggested that the electromagnetic field only responded to the surface eddy currents leaving the inner part of the body unmeasured [79]. The validity of the TOBEC method was also questioned in [79]. Unlike TOBEC, neither TRIM nor EMR was ever commercialized.

Magnetic induction tomography (MIT) provides a non-contact imaging of electrical properties of human tissue [80, 81]. A common MIT instrument consists of a large number of coils placed around the subject’s periphery. From the measured mutual inductance of the coil pairs, the subject’s conductivity distribution is attempted to be reconstructed to an image. In addition to the use of several coils, the imaging of low-conductivity objects has been shown to be

feasible also with a single coil acting simultaneously as source and detector [82]. Although MIT can be expected to be potential technology for the assessment of abdominal fat content, no publications advancing the method were found by the author at the time of writing. Instead, the method has been tried, e.g., for lung imaging [83].

1.4 Scope of the thesis

The aim of the thesis is to build a measuring instrument able to measure the rate of eddy current loss in human subjects at the height of the abdomen as a function of frequency, and to evaluate its capability to assess visceral fat accumulation. The appended publication [I] describes the developed measuring instrument, named as body electrical loss analysis (BELA), and reports the measured loss changing rates as a function of frequency in simple phantoms. In the appended publications [II] and [III] the BELA is tested in human subjects. First in ten subjects and then in thirty-eight subjects. For the study consisting the larger number of test subjects [III], the BELA prototype was improved and a new preamplifier described in [IV] was taken into use. Additionally, the appended publication [V] describes the developed open-source hardware for the tetra-polar electrical bioimpedance measurements. This hardware was used in [III] to measure the abdominal bioimpedance across the waist, to experiment if it would help to improve the BELA's correlation to VFA from what was obtained in [II].

2. Materials and Methods

2.1 Body electrical loss analysis (BELA)

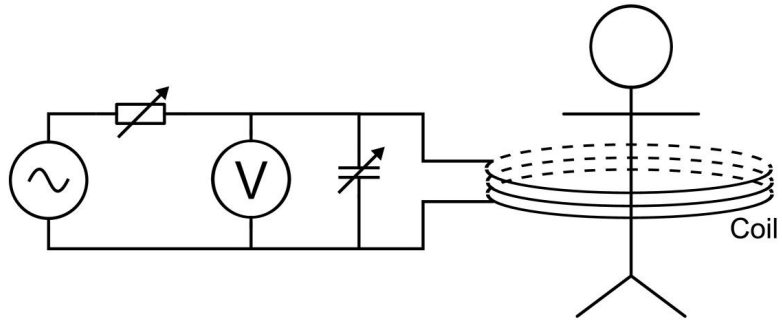


Figure 2.1. Simplified BELA instrumentation showing the coil as a part of the voltage divider circuitry.

The initial idea behind the BELA was first introduced in [84], where the measurement with a coil surrounding the abdomen was tested to estimate the accumulation of abdominal visceral fat. The simplified description of the method is illustrated in Figure 2.1 [I]. The coil, surrounding the abdomen, consists of tuned high-Q LC resonator connected to a voltage divider circuit. No contact electrodes are attached to the subject standing within the coil. The time-varying magnetic field \mathbf{B} produced by the coil induces so-called eddy currents in the abdomen. These currents oppose the applied field \mathbf{B} , and from the coil's point of view power is lost. For sinusoidal steady-state electromagnetic fields, the power loss due to the induced eddy currents in infinitesimal volume element dV is given by

$$dP = \sigma_{\text{eff}} E_{\text{rms}}^2 dV, \quad (2.1)$$

where σ_{eff} is the effective conductivity of tissue and E_{rms} is the root mean square value of the electric field \mathbf{E} at the point of a volume element dV [85, p. 35]. Furthermore, considering the human abdomen to be cylindrical in shape, and the changing magnetic field \mathbf{B} being applied perpendicular to base of the cylinder, the E_{rms} induced by the field \mathbf{B} is given by

$$E_{\text{rms}} = \frac{E_{\text{int}}}{\sqrt{2}} = \frac{\omega B r}{2\sqrt{2}}, \quad (2.2)$$

where E_{int} is the internal field \mathbf{E} circulating at distance r from the central axis of the cylinder, B is the strength of the field \mathbf{B} , and ω is the angular frequency of the field \mathbf{B} [85, p. 71]. Further, substituting $dV = 2\pi r h dr$ into Equation 2.1 and integrating over radius r yields to

$$P = \int_r \sigma_{\text{eff}} E_{\text{rms}}^2 2\pi r h dr \quad (2.3)$$

$$= \frac{\pi}{8} \sigma_{\text{eff}} \omega^2 B^2 r^4 h, \quad (2.4)$$

where r is the radius of the cylinder and h is the height of the cylinder. Equation 2.4 shows that higher tissue conductivity generates higher losses, i.e., lean body tissue that is electrically significantly more conductive than fat tissue loads the coil more (recall Table 1.2). Additionally, the losses get significantly larger with respect to radius, i.e., individuals with just a larger waist circumference load the coil more. However, tissue with low conductivity, such as fat, even if located at the outermost part of the abdomen, is not that lossy. Furthermore, instead of just measuring the losses, the novel idea behind BELA is to measure the rate of loss as the angular frequency of the magnetic field is increased [I]. The rate of loss is thought to give information on the conductivity of the interior of the abdomen. As shown in Figure 2.2, the abdominal area is considered to consist of three separate volumes: the interior (fatty or non-fatty), the muscles and the subcutaneous fat [II, III]. The influence of subcutaneous fat is considered

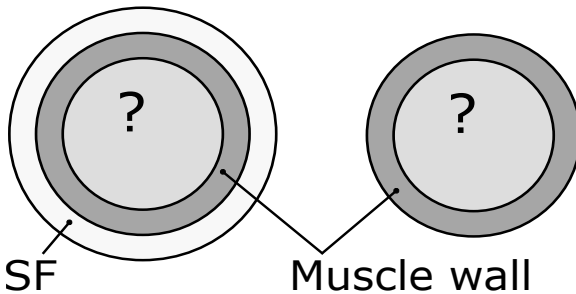


Figure 2.2. In the BELA measurement, the abdominal area is modelled to consist of three separate volumes in a cylinder-shaped container: the interior with the unknown conductivity, the highly conductive abdominal muscle wall, and the SF. From an electrical point of view, only the interior (fatty or non-fatty) and the surrounding volume of muscles are thought to interact in the measurement.

to be small because of its low conductivity. Removing the subcutaneous fat from the model, the model is reduced to consist of the interior with the unknown conductivity surrounded by the highly conductive layer of muscles. The lower the internal conductivity is, the faster the losses increase as the frequency increases. In the context of body composition, the loss changing rate was expected to be high in individuals with large amounts of visceral fat and vice versa.

2.1.1 Instrumentation

Two BELA prototypes were built, the first of which is shown in Figure 2.3. Eight turns of litz wire were wound on a wooden frame to form a rectangular helical coil (50 cm × 70 cm). The inductance L of the coil was approximately 110 μH . The second version, shown in Figure 2.4, consisted of a separate Helmholtz type of excitation coil in which the sensing coil (8 turns of litz wire) was placed. The shape of the coil was also changed from the rectangular of the first version to circular, having a diameter of 70 cm. The circular-shaped coil provided a more homogeneous field and allowed larger persons to fit into the coil. In both versions, the losses caused by the abdomen were measured at several resonant frequencies in the range from 100 kHz to 200 kHz. The frequency range of 100–200 kHz was selected partly because of practical reasons related to the used electronic components, but also because it is high enough to penetrate the cell membrane. At considerably lower frequencies the losses would have been generated mainly in the extracellular fluid only.

The losses, caused by the abdomen when placed in the coil, were measured as a change in the coil's impedance. At the resonant frequency, the coil's impedance for a high-Q unloaded coil is given by

$$Z = \frac{X^2}{R_{\text{loss}}} - jX, \quad (2.5)$$

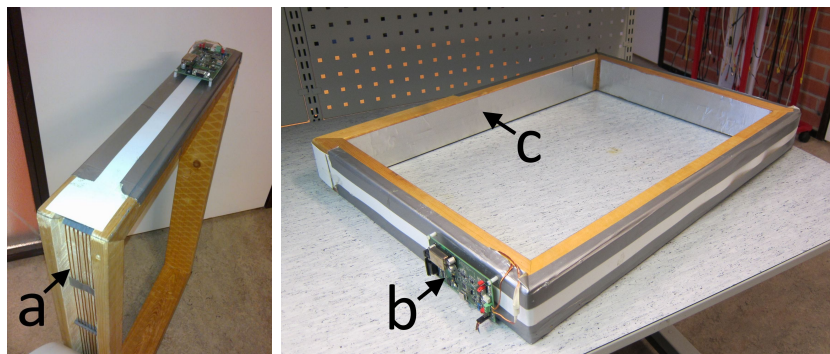


Figure 2.3. The first version of the BELA instrument consisted of eight turns of litz wire (a) wound around a wooden frame and connected to the measurement electronics (b). The grounded aluminium tape (c), covering the inner surface of the frame, added in [II], provides an electrostatic shield between the subject and the coil windings.

where R_{loss} is the equivalent ohmic loss resistance of the coil and X is the reactance, given by

$$X = \omega L = \frac{1}{\omega C}, \quad (2.6)$$

where $\omega = 1/\sqrt{LC} = 2\pi f_0$, f_0 being the resonant frequency, L is the inductance of



Figure 2.4. The second version of the BELA instrument used in [III]. The photograph (A) is taken at the Helsinki University Hospital, Meilahti. For the measurements, the coil was attached to a stand and connected to a laptop via a USB (Universal Serial Bus). Photograph (B) shows the coil winding under design. The aluminium frame also worked as an electrostatic shield as in [II]. The Figure is adapted by the author from [II].

the coil, and C is the capacitance of the tuning capacitor [I]. From Equation 2.5 it is worth noting that at the resonant frequency the coil's impedance is mainly resistive and is at its highest value. When the coil is loaded, i.e., R_{loss} is increased, the impedance Z decreases.

Figure 2.5 shows the front-end circuitry for the first and second versions. In the first version, the change in the coil's impedance was measured as an output voltage of the voltage divider. The divider was tuned to halve the excitation voltage at the resonant frequency. From Equations 2.5 and 2.6, the change in the output voltage of the voltage divider is approximately

$$\Delta V \approx V_0 \left(6 - 4 \frac{\omega L}{Q} \frac{1}{\Delta R_{\text{loss}}} \right)^{-1}, \quad (2.7)$$

where V_0 is the voltage applied across the voltage divider, Q is the quality factor of the empty coil, and ΔR_{loss} represents the ohmic equivalent loss resistance added by the subject loading the coil [I]. In the second prototype, ΔR_{loss} was measured as a change in the current circulating in the coil windings. This was done by using a current-sense transformer whose output voltage was measured. For an ideal 1:N current transformer the output voltage of the transformer is given by

$$V = I_p R_T / N, \quad (2.8)$$

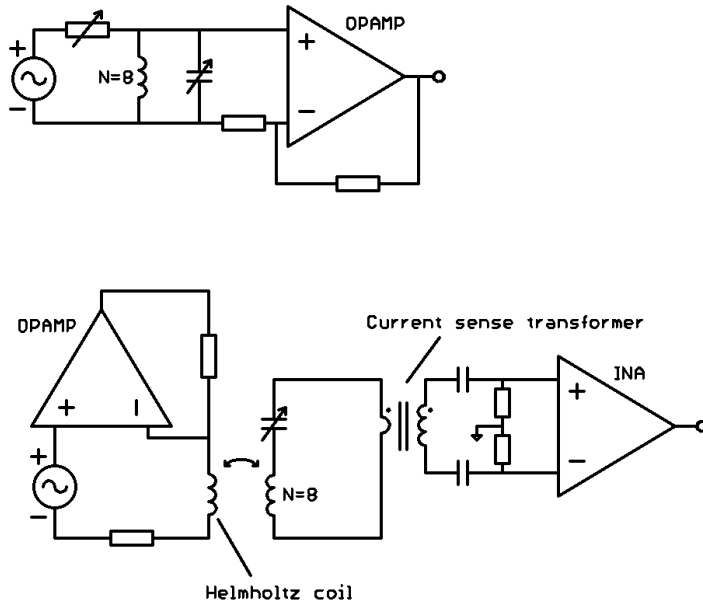


Figure 2.5. BELA sensor front-end. The circuit above is of the first version of the detector used in [I, II], and the one below is that of the second version used in [III]. Abbreviations: OPAMP, operational amplifier; INA, instrumentation amplifier; N, number of coil windings. Reprinted with permission.

where I_p is the primary current of the current transformer, N is the number of turns of the secondary winding, and R_T is a terminating resistor connected across the secondary winding [86].

Figure 2.6 shows the rest of the measurement electronics. The resonant frequency was sought with a frequency sweep, and it was changed by connecting a different sized capacitor in parallel with the coil. In the first version of the prototype this was done manually, whereas in the second version the change was automated by using relays. Phase sensitive detection, i.e., lock-in amplification, was used to measure both the real and imaginary parts of the voltage across the coil [I]. The active Sallen–Key low-pass filter (LPF) with its cut-off frequency set to around 1 kHz was used to convert the demodulated voltage across the coil to DC. The change in in-phase and quadrature-phase voltages were detected by a difference amplifier biased to the resonance voltage of an empty coil. In the second BELA prototype, the LPF and the difference amplifier were replaced with an amplifier topology based on the instrumentation amplifier (INA) shown in Figure 2.7 [IV]. The new design also provided the second-order LPF followed by the difference amplifier but in a single active stage with less external passive components and smaller routing area. This allowed increasing the measurement speed, as due to reduced electrical noise it was possible to lower the number of consecutive frequency sweeps (averaging) from 16–32 to 4. The amplifier’s

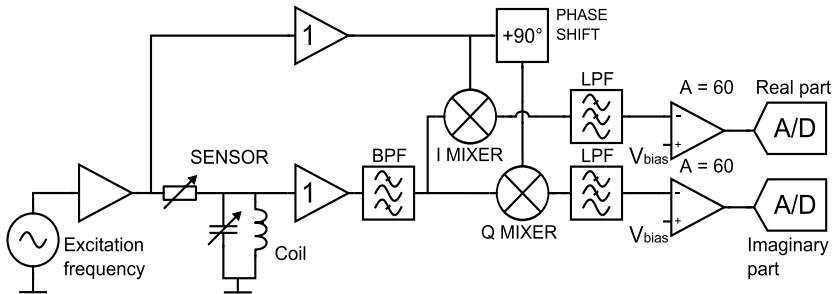


Figure 2.6. BELA measurement electronics from excitation to analog-to-digital conversion. Abbreviations: BPF, band-pass filter; LPF, low-pass filter; I, in-phase; Q, quadrature-phase; A, amplification; A/D, analog-to-digital converter.

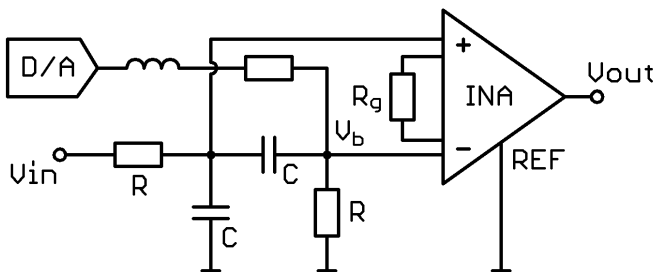


Figure 2.7. A second-order active low-pass filter to simultaneously provide a high gain factor and DC voltage subtraction [IV]. Abbreviations: D/A, digital-to-analog converter; V_b , bias voltage; R_g , gain resistor, REF, reference.

ability to work as a 2-pole active filter, and its stability with 40 dB gain was verified in [IV] for Analog Devices' AD8221 and Linear Technology's LT1920.

2.2 Study I: Experiments with phantoms

In study [I], the idea behind the BELA method was tested with phantoms shown in Figure 2.8. The conductivity of the saline and the sunflower oil, used in phantoms, were approximately 2 S/m and 0.2 mS/m, respectively.

2.2.1 BELA measurement

The phantoms were placed in the coil, and the change in the voltage across the coil was measured at five different excitation frequencies from 100 kHz to 200 kHz. Both in-phase and quadrature-phase voltages were measured. The measurements were repeated ten times at every frequency. For each measurement the coil was recalibrated as empty before the phantom was put back into the coil.

2.3 Study II: Feasibility in human subjects

In study [III], BELA's ability to assess abdominal visceral fat was tested for the first time. Ten healthy volunteers (5 males, 5 females, age: 22–60 years) covering the BMI range of 21–30 kg/m² and the waist circumference range of 73–108 cm were recruited from laboratory personnel and acquaintances. All volunteers were measured with the BELA instrument and imaged with MRI within one week. Furthermore, the BELA measurement was repeated for one subject on three consecutive days. The effect of the standing position within the BELA was also tested in one test subject. The coordinating ethics committee of Helsinki University Central Hospital approved the study, and an informed written consent was taken from the volunteers.

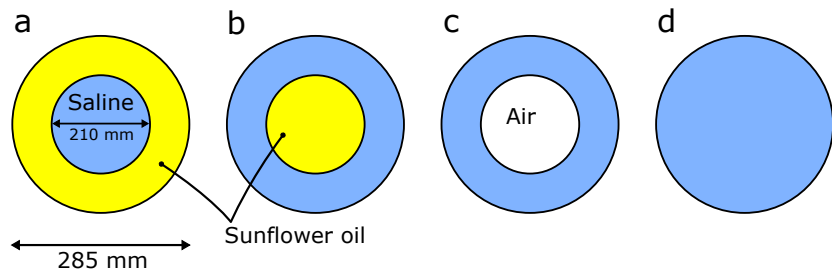


Figure 2.8. Test phantoms placed in the BELA instrument. Phantoms (a) and (b) had reversed conductivity distributions, (c) had a similar structure to (b) but with a less lossy interior, and (d) was homogeneous. All the phantoms were of the same size.

2.3.1 BELA measurement

The first BELA prototype version was used. The measurements were taken in a standing position at 103 kHz and 185 kHz. Three different levels of the abdomen were measured: the navel, navel +5 cm and navel -5 cm. The measurements were repeated five times at every level and frequency. On changing the frequency, the test subject had to exit the coil when calibrating the instrument. Only in-phase voltages were used in analysis.

2.3.2 Quantification of fat distribution

The fat distribution was measured on a clinical 1.5-Tesla MR imager (Avanto, Siemens, Erlangen, Germany) using a T1-weighted gradient echo sequence with selective fat excitation. A stack of sixteen axial image slices with a nominal thickness of 1 cm was centered at the L4–L5 intervertebral disk [II]. The MR images were analyzed using a segmentation algorithm (SliceOmatic v4.3, TomoVision, Magog, Quebec, Canada). The VFA and SFA were determined at the level of umbilicus.

2.3.3 Statistical analysis

The statistical relationship of BELA to VFA and SFA were studied using linear regression and correlation analysis [87, p. 75–79]. The coefficient of determination (R^2) was reported for VFA, SFA, VFA/SFA, and SFA/VFA, as well as for BMI and waist circumference. A p -value <0.05 was considered to be statistically significant. To estimate the agreement between the BELA and MRI, SEE and leave-one-out cross-validation (LOOCV) were calculated. The repeatability of the BELA was estimated using

$$\Delta m_{\text{loss}} = \frac{\sigma_H + \sigma_L}{f_H - f_L}, \quad (2.9)$$

where Δm_{loss} is the deviation in the measured rate of loss over five BELA measurements, σ_H and σ_L are the standard deviations of the measured voltage changes across the coil at high and low frequencies, f_H and f_L , respectively.

2.4 Study III: Clinical trial on human participants

In study [III], the BELA's ability to assess abdominal visceral fat was evaluated against MRI in thirty-eight volunteers (17 males, 21 females) covering the age range of 20–68 years, the BMI range of 19.6–39.4 kg/m², and the waist circumference range of 78–128 cm. The mean BMI was 27.09 ± 4.79 kg/m², whereas the mean waist circumference was 96.5 ± 11.0 cm for men and 94.7 ± 12.9 cm for women. In addition to BELA and MRI, all volunteers underwent also single-frequency abdominal impedance (SAI) and BIA measurements. All

the measurements were conducted consecutively. The comparison to MRI was studied by including all test subjects, as well as separately in men and women, and in subjects with BMI ≤ 27 and > 27 kg/m². Additionally, BELA and BIA were compared to waist circumference and the circumference of muscles estimated from the measured SAI.

All volunteers were recruited from acquaintances and from the Obesity Research Unit of University of Helsinki. The volunteers were instructed not to eat during four hours before the measurement. However, water intake was allowed. The coordinating ethics committee of Helsinki University Hospital approved the study and the volunteers gave an informed written consent.

2.4.1 BELA measurement

The second version of the BELA prototype was used. The measurements were carried out in a standing position at three frequencies: 110 kHz, 155 kHz and 194 kHz. Similarly as in [II], three different measurement heights, the umbilicus level, umbilicus +5 cm and umbilicus -5 cm were used. Before the test subject was instructed to enter the coil, the instrument was calibrated for every frequency and the calibration measurements were stored in the device memory. The subject did not have to exit the coil between the frequency change.

2.4.2 Bioelectrical impedance analysis

A commercial body-fat scale OMRON BF-508 with hand grips was used to measure the visceral fat level. The measurement was carried out in a standing position as instructed in the device manual. Before each measurement the subject's age, gender, and height were entered via the scale's user interface. A guest mode, that does not store data in the device memory after the measurements, was used. Electrode contact areas were also cleaned between the measurements with a small amount of 70% isopropyl alcohol.

2.4.3 Single-frequency abdominal impedance (SAI)

The SAI was used to estimate the abdominal muscle wall circumference, i.e., the BELA effective waist circumference, given by

$$WC_{\text{eff}} = WC - 2\pi \text{SFL}, \quad (2.10)$$

where WC is the measured waist circumference and SFL is subcutaneous fat layer thickness estimated from the measured SAI at 50 kHz [88] as

$$\text{SFL (mm)} = 0.89 \text{SAI}_{50} - 10.84. \quad (2.11)$$

The measurement was taken in standing position using OpenEBI [V] measuring instrument shown in Figure 2.9. Four Dura-Stick Plus self-adhesive electrical stimulation electrodes (DJO Global, Inc., Vista, CA, USA), also shown



Figure 2.9. OpenEBI measurement electronics [V] and a pair of self-adhesive 5 x 9 cm rectangular silver/silver chloride (Ag/AgCl) electrodes.

in Figure 2.9, were placed across the waist as in [V], i.e., current and voltage electrodes on each flank approximately 1.5–2 cm away from each other. A small amount of 70% isopropyl alcohol was used to prepare the skin for the electrode placement.

In the design of the OpenEBI, care was taken to choose both the output and input impedances so that no more than a 1% error would be introduced in the measurement [V]. For a 2R-1C biological tissue equivalent circuit, the observed relative error in the impedance was $-0.73 \pm 0.34\%$ in the range from 10 kHz to 100 kHz. Furthermore, for two test subjects having waist circumferences 98 cm and 109 cm, the magnitude of the abdominal impedances were 20 Ω and 60 Ω , respectively [V]. These impedance values match in magnitude with the impedance values observed in [88]. Finally, safety issues were also considered by measuring the amplitude of the OpenEBI output current. During the frequency sweep from 4 kHz to 100 kHz, the RMS current was approximately 175 μA [V]. The DC current was 0.36 μA at most during the frequency sweep, except for a short 16 μA transient peak at the beginning of the sweep.

2.4.4 Quantification of fat distribution

The fat distribution was measured on a clinical 1.5-Tesla MR imager (Avanto, Siemens, Erlangen, Germany). The same approach was used as in [II], but this time also the volumes of visceral and subcutaneous fat, VFV and SFV, respectively, were quantified.

2.4.5 Statistical analysis

The statistical relationship of BELA to the visceral and subcutaneous fat depot sizes, were studied using linear regression and correlation analysis. The data was analyzed similarly as in [II], but instead of R^2 the Pearson correlation coefficient, r , was reported. The strength of r was interpreted as shown in Table 2.1.

Table 2.1. An interpretation of the strength of r used through this work.

r	Interpretation
< 0.5	Weak
0.50–0.64	Modest
0.65–0.74	Moderate
0.75–0.84	Moderately strong
0.85–0.94	Strong
≥ 0.95	Very strong

3. Results

3.1 Study I: Experiments with phantoms

Figure 3.1 shows the measured voltage changes for in-phase and quadrature-phase signals at different resonant frequencies when the coil was loaded by phantoms A and B. The loss changing rate calculated from the in-phase signals were approximately 0.14 mV/kHz and 0.41 mV/kHz for phantoms A and B, respectively. Similarly, Figure 3.2 shows the measured voltage changes at different resonant frequencies for phantoms C and D. The respective signal slopes were approximately 0.47 mV/kHz and 0.73 mV/kHz. The mean value of the quadrature-phase signals were close to zero for every measured phantom.

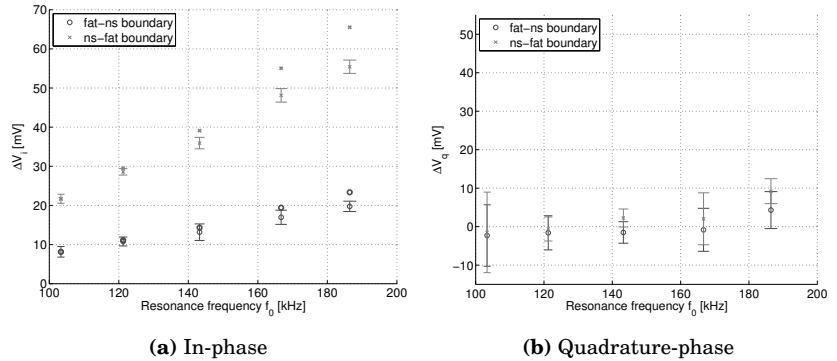


Figure 3.1. Phantoms A and B with the boundaries of fat-normal saline (circles) and normal saline-fat (crosses) measured at different frequencies. The error bars represent the standard deviation over ten consecutive measurements. The points in boldface are the mean values multiplied by the compensation factor k introduced in [1].

Results

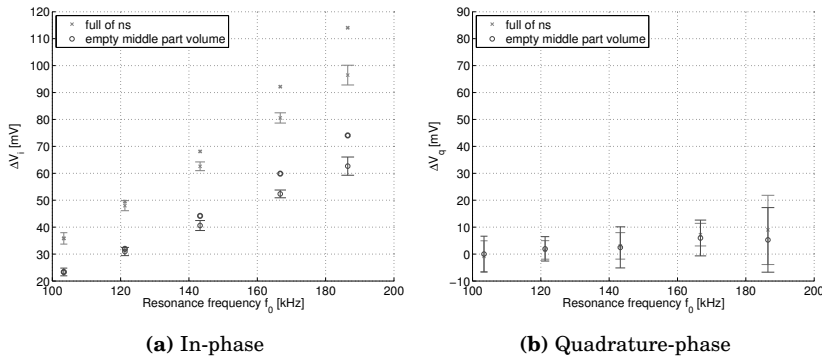


Figure 3.2. Same as Figure 3.1 but for phantoms C and D with air core (circles) and full of normal saline (crosses).

3.2 Study II: Feasibility in human subjects

A strong correlation, $R^2 = 0.74$ with $SEE = 29.7 \text{ cm}^2$ and $LOOCV = 40.1 \text{ cm}^2$, was found between the VFA obtained with MRI and the loss changing rate measured at the level of umbilicus +5 cm (Figure 3.3). At the level of the umbilicus, the correlation to VFA was considerably weaker ($R^2 = 0.43$). No statistically significant correlation to VFA was found at the level of umbilicus -5 cm. Neither was there a correlation between the SFA obtained with the MRI and the loss changing rate measured either at the level of the umbilicus, umbilicus +5 cm or umbilicus -5 cm. One of the volunteers had an exceptionally large amount of visceral fat and thus was excluded from the analysis (Figure 3.4).

The average estimate of repeatability of the BELA signal observed through the study was $\pm 9.6\%$. The loss changing rates measured in three consecutive days in one test subject were $0.60 \pm 0.03 \text{ mV/kHz}$, $0.61 \pm 0.01 \text{ mV/kHz}$, and $0.57 \pm 0.01 \text{ mV/kHz}$ (mean \pm standard deviation) at the level of the umbilicus, umbilicus +5 cm, and umbilicus -5 cm, respectively. The effect of the standing position on the measured loss changing rate in one test subject was $\pm 2.5\%$ at f_L and $\pm 1.5\%$ at f_H .

3.3 Study III: Clinical trial on human participants

Figure 3.5 shows the correlation of BELA and BIA to VFA and SFA as well as to VFV and SFV in all subjects. There was no significant difference whether the correlation was studied by using the VFA or VFV. The strongest correlation of BELA to VFA in all subjects was found at the height of umbilicus +5 cm ($r = 0.61$, $SEE = 59.30$), and it tended to decrease when the measurement height was lowered. The correlation to SFA at the height of umbilicus +5 cm was $r = 0.43$ (weaker is better), and it tended to increase when the measurement height was lowered. In subjects with $BMI \leq 27 \text{ kg/m}^2$ there was no correlation

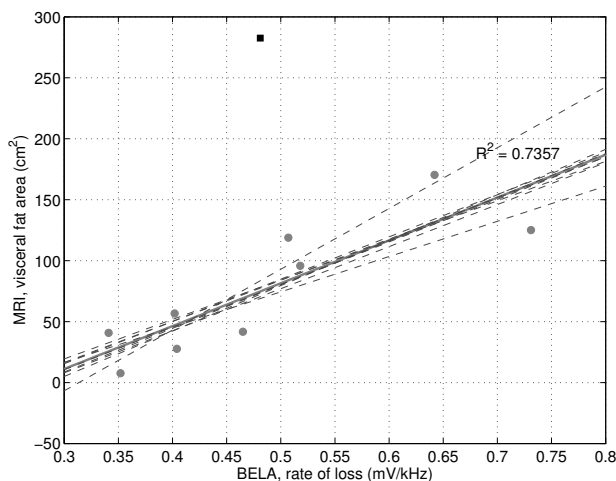


Figure 3.3. Linear regression between the VFA obtained with MRI and the loss changing rate measured at the umbilicus +5 cm in nine volunteers who took part in the study [II]. Dashed lines are multiple regression lines of leave-one-out style cross validation. The measurement marked with ■ was of a volunteer who had an exceptionally large amount of abdominal visceral fat and thus was excluded from the analysis.

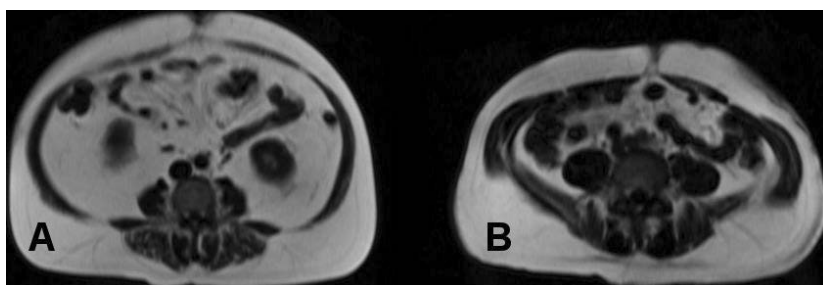


Figure 3.4. Volunteer A who took part in the study [II] had an exceptionally large amount of abdominal visceral fat but a smaller amount of subcutaneous fat than volunteer B whose VFA was at a reasonable level. The relative amount of conductive tissue (muscles) compared with poorly conductive fatty tissue was so small in A that the BELA was not able differentiate the VFA from the SFA.

between BELA and VFA, and in women the correlation to SFA was unexpectedly strong, $r = 0.89$ with $SEE = 61.75$. The correlation of BIA to VFA in all subjects was $r = 0.70$ with $SEE = 53.43$, and it equalled to SFA with $SEE = 93.78$. In comparison to BELA, BIA tended to correlate more evenly with VFA across different subgroups.

Figure 3.6 demonstrates when the subject's cross-sectional image fitted well with its respective electrical body model and when it does not. Furthermore, Figure 3.7 shows the correlation of BELA and BIA to WC and WC_{eff} estimated from the measured SFL. Although, there was a strong correlation between the BELA and WC_{eff} , $r = 0.86$ – 0.90 , using the WC_{eff} as a scaling factor for BELA did not help to improve its correlation to VFA.

Results

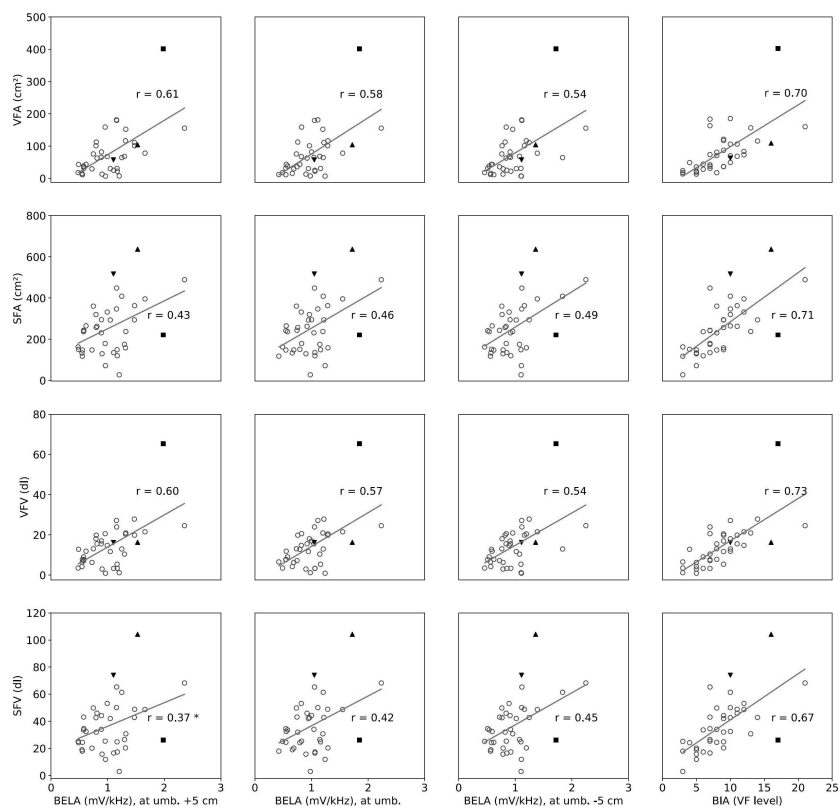


Figure 3.5. Linear regression of BELA and BIA on visceral and subcutaneous fat area as well as on their respective volumes. The cross-sectional MR images of subject ▼, ▲ and ■ are shown in Figure 3.6 as A, B and C, respectively. Reprinted with permission.

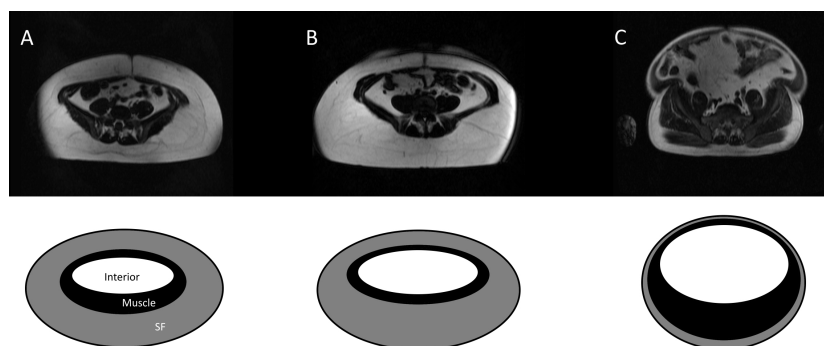


Figure 3.6. Cross-sectional MR image fitted to its respective body model from an electrical point of view. The electrical body model fit well with subject A and B. Reprinted with permission.

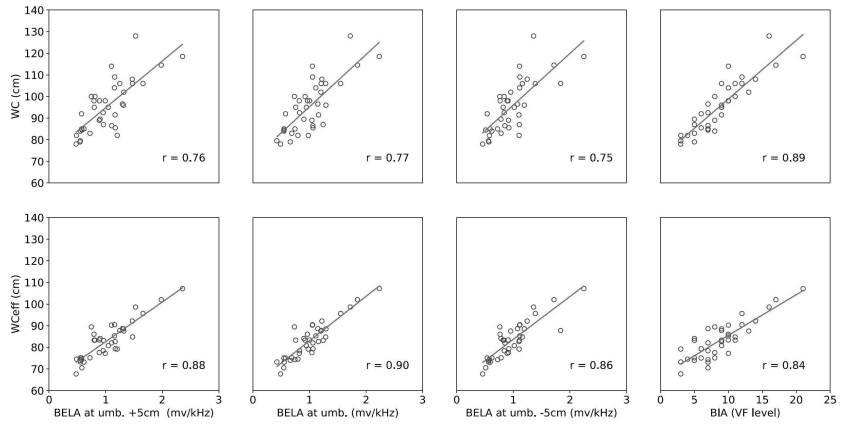


Figure 3.7. Linear regression of BELA and BIA on WC and WC_{eff} . Reprinted with permission.

Results

4. Discussion

The primary motivation for research on BELA has been to develop a simple and inexpensive method to assess visceral fat that is in good agreement with MRI. Waist circumference is arguably the most widely used surrogate for assessing abdominal visceral fat accumulation. It is simple, extremely cost-effective and has a moderately strong correlation to VFA. Thus, any new method to be adopted in clinical practice has to provide significant improvement over waist circumference. The costs of the new method may be higher as long as the method is accurate. However, the method should not require medical personnel to perform the measurement or interpret the results.

First BELA was tested with simple phantoms [I]. The results of the study suggested that the idea of loss changing rate measured by BELA is sound and worth testing in human participants to assess the accumulation of abdominal visceral fat. In nine subjects recruited from laboratory personnel and acquaintances, a strong relationship between the BELA, measured at the height of umbilicus +5 cm, and the VFA obtained with MRI was found [II]. However, further studies in thirty-eight subjects [III] showed only a modest relationship between the VFA and BELA. Also, the large SEE value suggested a poor agreement with MRI. Thus, the strong correlation obtained in [II] seems to have been obtained by chance. A possible reason for this may be that due to practicalities in [II], the subjects were measured with the BELA and MRI approximately one week apart, whereas in [III] both BELA and MRI were measured in one session.

BELA is a bioimpedance-based method, and in this work it has been compared to BIA. Most of the BIA studies have been conducted by using the commercially available InBody 720 body composition analyzer. However, today many body-fat scales (i.e. 'bathroom-BIA') which previously measured only the fat percentage gives an estimate for visceral fat too. Thus in [III], it was decided to measure the visceral fat also with the 'bathroom-BIA'. In agreement with [20, 63], BIA's ability to measure visceral fat accurately is yet to achieve that of reference techniques. Although BIA correlated better with VFA than BELA, the correlation was not considered significantly better. Furthermore, some studies [57, 58] have found almost the exact same correlation between the VFA and BIA that was obtained for BELA. Moreover, BIA was found to correlate equally strongly with

SFA, whereas BELA's correlation to SFA was weak. The weaker correlation to SFA is considered better as it suggests the measurement is less affected by subcutaneous fat. Finally, unlike BIA, BELA did not rely on any statistical age, sex or additional anthropometry in its analysis.

Combining BELA with the abdominal bioimpedance across the waist, i.e. SAI, was also tested. SAI was believed to help BELA in its estimation of VFA from the measured loss changing rate, especially in subjects with diastasis. Like in [65], the abdominal bioimpedance measured in [III] was found to correlate moderately strongly with SFA. The results are also in agreement with [88], where the abdominal bioimpedance was found to correlate very strongly with the abdominal subcutaneous fat layer thickness measured from MRI. However, instead of gaining any improvement in the correlation of BELA to VFA, BELA was found to correlate strongly with the circumference of the abdominal muscle wall estimated from the SAI and the subject's waist circumference. Eddy current losses are known to be heavily dependent on the circumference of the outermost conductive layer, but in this regard the result was not expected since the fairly homogeneous conductive layer of muscles is part of the analysis. Without the conductive layer of muscles surrounding the unknown interior, the idea of the internal conductivity measurement by the loss changing rate is not sound. In terms of VFA, the study cohort in [III] consisted of a large sample of different internal conductivity levels (10–200 cm²), which when taken into account, seems to indicate that the BELA has fundamental limitations to probe the VFA.

The results of this work strengthen the critical observation that the measurement of bulk impedance is not optimal for predicting VFA. Similar results can be achieved with the anthropometric measurements only, such as by using waist circumference. It is confusing that some studies have reported a strong relationship between the VFA observed by using an imaging technique and the VFA estimated by exploiting an impedance method, whereas others conclude that the impedance method is the least accurate. In [65], a strong correlation was reported between the VFA and the abdominal BIA. However, the exclusion of the impedance from the prediction equation resulted in almost exactly the same correlation. Similarly, combining abdominal BIA with the measurement of waist circumference [64] is yet to prove its value to the use of waist circumference alone [89].

Although the envisioned accuracy of BELA to detect abdominal visceral fat was not achieved, this work is considered to help guide future studies on bioimpedance-based methods. A completely new parameter to measure body composition, the loss changing rate, was introduced. Additionally, the strong relationship between the BELA and the circumference of the abdominal wall muscles suggest potential in other applications of body composition, e.g., to estimate the boundary of abdominal subcutaneous fat [72]. Regarding the measurement of VFA with BELA, the following uncertainties have been noticed and should be considered in possible follow-up studies. The measurement position, which was overlooked in [II] and [III], may have caused confusion in the analysis.

The BELA measurement was taken in the standing position, but in the MRI the test subjects were lying in the supine position. This may have had some effect on the bioelectrical anisotropy of body tissues and thus to the amount of VFA calculated from the MRI compared to the VFA estimated by BELA. To avoid this uncertainty, BELA could be measured in the supine position as well. Additionally, in [III], the correlation of BELA to SFA was found to be strong in women. The subjects were not asked about their recent eating habits, so it is possible that some of them were on a diet which may have increased the electrical conductivity of their subcutaneous fat due to its increased water content, as it was found in [90]. Thus the water content in the subcutaneous fat should be controlled.

Discussion

5. Conclusion

A new bioimpedance-based measurement method, BELA, aimed at measuring abdominal visceral fat was developed and evaluated. The results suggest that, in its current form, BELA is not accurate enough to be used to estimate abdominal visceral fat in clinical settings. In the evaluation cohort consisting of thirty-eight volunteers, the correlation between the VFA obtained with MRI and the VFA estimated by BELA was not considered strong enough to suggest obtaining a prediction formula for VFA using regression from BELA and MRI. Instead, BELA was found to correlate strongly with the circumference of the abdominal wall muscles estimated from the waist circumference and subcutaneous fat layer thickness measured with SAI.

Being a bioimpedance-based method, BELA was compared to BIA. For the same evaluation cohort, BIA was not considered to perform significantly better. In addition to bioimpedance, the BIA also included statistical gender, age and BMI in its analysis, whereas BELA relied on impedance only. The results of this study strengthen the critical observation that the measurement of bulk impedance is not optimal to predict abdominal visceral fat. Similar results can be achieved with the anthropometric measurements only, such as by using waist circumference.

Conclusion

References

- [1] World Health Organization. Fact sheet 311 – Obesity and overweight. <http://www.who.int/mediacentre/factsheets/fs311/en/>, 2018. Accessed 23 Feb. 2018.
- [2] F. Q. Nuttall. Body mass index: Obesity, BMI, and health: a critical review. *Nutrition Today*, 50(3):117–128, 2015.
- [3] J-P. Després and B. Lamarche. Effects of diet and physical activity on adiposity and body fat distribution: implications for the prevention of cardiovascular disease. *Nutrition Research Reviews*, 6(1):137–159, 1993.
- [4] R. S. Ahima and M. A. Lazar. The health risk of obesity—better metrics imperative. *Science*, 341(6148):856–858, 2013.
- [5] T. F. Teixeira, R. D. Alves, A. P. Moreira, and M. do C. Peluzio. Main characteristics of metabolically obese normal weight and metabolically healthy obese phenotypes. *Nutrition in Clinical Care*, 73(3):175–190, 2015.
- [6] U. Gurunathan and P. S. Myles. Limitations of body mass index as an obesity measure of perioperative risk. *British Journal of Anaesthesia*, 116(3):319–321, 2016.
- [7] R. M. Puhl and C. A. Heuer. The stigma of obesity: a review and update. *Obesity*, 17(5):941–964, 2009.
- [8] L. Laforest, E. Van Ganse, C. Ritleng, G. Desamericq, L. Letrilliart, A. Moreau, S. Rosen, H. Mechin, and G. Chamba. Correlates of quality of life of pre-obese and obese patients: a pharmacy-based cross-sectional survey. *BMC Public Health*, 9(337), 2009.
- [9] R. P. Wildman, P. Muntner, K. Reynolds, A. P. McGinn, S. Rajpathak, J. Wylie-Rosett, and M. R. Sowers. The obese without cardiometabolic risk factor clustering and the normal weight with cardiometabolic risk factor clustering: prevalence and correlates of 2 phenotypes among the US population (NHANES 1999–2004). *Archives of Internal Medicine*, 168(15):1617–1624, 2008.
- [10] A. J. Tomiyama, J. M. Hunger, J. Nguyen-Cuu, and C. Wells. Misclassification of cardiometabolic health when using body mass index categories in NHANES 2005–2012. *International Journal of Obesity*, 40(5):883–886, 2016.
- [11] The U.S. Equal Employment Opportunity Commission (EEOC). Regulations under the Americans with disabilities act. *Federal Register*, 81(95):31126–31143, 2016.
- [12] R. N. Bergman, S. P. Kim, K. J. Catalano, I. R. Hsu, J. D. Chiu, M. Kabir, K. Hucking, and M. Ader. Why visceral fat is bad: mechanisms of the metabolic syndrome. *Obesity*, 14(S2):16S–19S, 2006.

- [13] R. V. Shah, V. L. Murthy, S. A. Abbasi, R. Blankstein, R. Y. Kwong, A. B. Goldfine, M. Jerosch-Herold, J. A. Lima, J. Ding, and M. A. Allison. Visceral adiposity and the risk of metabolic syndrome across body mass index: the MESA study. *JACC: Cardiovascular Imaging*, 7(12):1236–1238, 2014.
- [14] C. Eipel, K. Abshagen, and B. Vollmar. Regulation of hepatic blood flow: the hepatic arterial buffer response revisited. *World Journal of Gastroenterology*, 16(48):6046–6057, 2010.
- [15] S. A. Porter, J. M. Massaro, U. Hoffmann, R. S. Vasan, C. J. O'Donnel, and C. S. Fox. Abdominal subcutaneous adipose tissue: a protective fat depot? *Diabetes Care*, 32(6):1068–1075, 2009.
- [16] M. Zhang, T. Hu, S. Zhang, and L. Zhou. Associations of different adipose tissue depots with insulin resistance: a systematic review and meta-analysis of observational studies. *Scientific Reports*, 21(5):18495, 2015.
- [17] S. K. Fried, M-J. Lee, and K. Karastergiou. Shaping fat distribution: new insights into the molecular determinants of depot- and sex-dependent adipose biology. *Obesity*, 23(7):1345–1352, 2015.
- [18] H. Kwon, D. Kim, and J. S. Kim. Body fat distribution and the risk of incident metabolic syndrome: a longitudinal cohort study. *Scientific Reports*, 7(1):10955, 2017.
- [19] E. L. Thomas, J. R. Parkinson, G. S. Frost, A. P. Goldstone, C. J. Doré, J. P. McCarthy, A. L. Collins, J. A. Fitzpatrick, G. Durighel, S. D. Taylor-Robinson, and J. D. Bell. The missing risk: MRI and MRS phenotyping of abdominal adiposity and ectopic fat. *Obesity*, 20(1):76–87, 2012.
- [20] A. Shuster, M. Patlas, J. H. Pinthus, and M. Mourtzakis. The clinical importance of visceral adiposity: a critical review of methods for visceral adipose tissue analysis. *The British Journal of Radiology*, 85(1009):1–10, 2012.
- [21] B. J. Klopfenstein, M. S. Kim, C. M. Krisky, J. Szumowski, W. D. Rooney, and J. Q. Purnell. Comparison of 3 T MRI and CT for the measurement of visceral and subcutaneous adipose tissue in humans. *The British Journal of Radiology*, 85(1018):e826–e830, 2012.
- [22] T. Gomi, Y. Kawawa, M. Nagamoto, H. Terada, and E. Kohda. Measurement of visceral fat/subcutaneous fat ratio by 0.3 Tesla MRI. *Radiation medicine*, 23(8):584–7, 2006.
- [23] M. Warren, P. J. Schreiner, and J. G. Terry. The relation between visceral fat measurement and torso level—is one level better than another? The atherosclerosis risk in communities study, 1990–1992. *American Journal of Epidemiology*, 163(4):352–358, 2006.
- [24] H. H. Hu, J. Chen, and W. Shen. Segmentation and quantification of adipose tissue by magnetic resonance imaging. *Magnetic Resonance Materials in Physics, Biology and Medicine*, 29(2):259–276, 2016.
- [25] V. R. Preedy, editor. *Handbook of anthropometry: physical measures of human form in health and disease*. Springer-Verlag New York, 2012.
- [26] Y. Matsuzawa. Metabolic syndrome—definition and diagnostic criteria in Japan. *Journal of Atherosclerosis and Thrombosis*, 12(6):301–301, 2005.
- [27] Y. Matsuzawa, T. Funahashi, and T. Nakamura. The concept of metabolic syndrome: Contribution of visceral fat accumulation and its molecular mechanism. *Journal of Atherosclerosis and Thrombosis*, 18(8):629–639, 2011.

- [28] T. Rankinen, S-Y. Kim, L. Pérusse, J-P. Després, and C. Bouchard. The prediction of abdominal visceral fat level from body composition and anthropometry: ROC analysis. *International Journal of Obesity*, 23(8):801–809, 1999.
- [29] J. L. Kuk, T. S. Church, S. N. Blair, and R. Ross. Does measurement site for visceral and abdominal subcutaneous adipose tissue alter associations with the metabolic syndrome? *Diabetes Care*, 29(3):679–684, 2006.
- [30] C. V. Albanese, E. Diessel, and H. K. Genant. Clinical applications of body composition measurements using DXA. *Journal of Clinical Densitometry*, 6(2):75–85, 2003.
- [31] A. Bazzocchi, F. Ponti, U. Albisinni, G. Battista, and G. Guglielmi. DXA: Technical aspects and application. *European Journal of Radiology*, 85(8):1481–1492, 2016.
- [32] C. V. Albanese, E. Diessel, and H. K. Genant. Ultrasound: Which role in body composition? *European Journal of Radiology*, 85(8):1469–1480, 2016.
- [33] G. M. Blake and I. Fogelman. The role of DXA bone density scans in the diagnosis and treatment of osteoporosis. *Postgraduate Medical Journal*, 83(982):509–517, 2007.
- [34] I. J. Neeland, S. M. Grundy, X. Li, B. Adams-Huet, and G. L. Vega. Comparison of visceral fat mass measurement by dual-X-ray absorptiometry and magnetic resonance imaging in a multiethnic cohort: the Dallas Heart Study. *Nutrition & Diabetes*, 6(7):e221, 2016.
- [35] K. Meredith-Jones, J. Haszard, N. Stanger, and R. Taylor. Precision of DXA-derived visceral fat measurements in a large sample of adults of varying body size. *Obesity*, 26(3):505–512, 2018.
- [36] F. Armellini, M. Zamboni, L. Rigo, T. Todesco, I. A. Bergamo-Andreis, C. Procacci, and O. Bosello. The contribution of sonography to the measurement of intra-abdominal fat. *Journal of Clinical Ultrasound*, 18(7):563–567, 1990.
- [37] A. Bazzocchi, G. Filonzi, F. Ponti, C. Sassi, E. Salizzoni, G. Battista, and R. Canini. Accuracy, reproducibility and repeatability of ultrasonography in the assessment of abdominal adiposity. *Academic Radiology*, 18(9):1133–1143, 2011.
- [38] T. Miazgowski, R. Kucharski, M. Soltysiak, A. Taszarek, B. Miazgowski, and K. Widecka. Visceral fat reference values derived from healthy European men and women aged 20–30 years using GE Healthcare dual-energy x-ray absorptiometry. *PLOS ONE*, 12(7):1–11, 2017.
- [39] M-C. Pouliot, J-P. Després, S. Lemieux, S. Moorjani, C. Bouchard, A. Tremblay, A. Nadeau, and P. J. Lupien. Waist circumference and abdominal sagittal diameter: Best simple anthropometric indexes of abdominal visceral adipose tissue accumulation and related cardiovascular risk in men and women. *The American Journal of Cardiology*, 73(7):460–468, 1994.
- [40] M. Zamboni, E. Turcato, F. Armellini, H. S. Kahn, A. Zivelonghi, H. Santana, I. A. Bergamo-Andreis, and O. Bosello. Sagittal abdominal diameter as a practical predictor of visceral fat. *International Journal of Obesity*, 22(7):655–660, 1998.
- [41] A. Bosy-Westphal, C-A. Booke, T. Blöcker, E. Kossel, K. Goele, W. Later, B. Hitze, M. Heller, C-C. Glüer, and M. J. Müller. Measurement site for waist circumference affects its accuracy as an index of visceral and abdominal subcutaneous fat in a Caucasian population. *The Journal of Nutrition*, 140(5):954–961, 2010.
- [42] J. Wang, J. C. Thornton, S. Bari, B. Williamson, D. Gallagher, S. B. Heymsfield, M. Horlick, D. Kotler, B. Laferrère, L. Mayer, F. X. Pi-Sunyer, and R. N. Pierson Jr. Comparisons of waist circumferences measured at 4 sites. *The American Journal of Clinical Nutrition*, 77(2):379–384, 2003.

- [43] S. K. Agarwal, A. Misra, P. Aggarwal, A. Bardia, R. Goel, N. K. Vikram, J. S. Wasir, N. Hussain, K. Ramachandran, and R. M. Pandey. Waist circumference measurement by site, posture, respiratory phase, and meal time: implications for methodology. *Obesity*, 17(5):1056–1061, 2009.
- [44] J. Medina-Inojosa, V. K. Somers, T. Ngwa, L. Hinshaw, and F. Lopez-Jimenez. Reliability of a 3D body scanner for anthropometric measurements of central obesity. *Obesity, Open Access*, 2(3), 2016.
- [45] S. B. Heymsfield, B. Bourgeois, B. K. Ng, M. J. Sommer, X. Li, and J. A. Shepherd. Digital anthropometry: a critical review. *European Journal of Clinical Nutrition*, 72:680–687, 2018.
- [46] World Health Organization. *Waist circumference and waist-hip ratio: report of WHO expert consultation, Geneva, 8–11 December 2008*. WHO Document Production Services, Geneva, Switzerland, 2011; 1–39.
- [47] K. van der Kooy, R. Leenen, J. C. Seidell, P. Deurenberg, A. Droop, and C. J. Bakker. Waist-hip ratio is a poor predictor of changes in visceral fat. *The American Journal of Clinical Nutrition*, 57(3):327–333, 1993.
- [48] P. F. Rønn, G. S. Andersen, T. Lauritzen, D. L. Christensen, M. Aadahl, B. Carstensen, and M. E. Jørgensen. Ethnic differences in anthropometric measures and abdominal fat distribution: a cross-sectional pooled study in Inuit, Africans and Europeans. *Journal of Epidemiology & Community Health*, 71(6):536–543, 2017.
- [49] K. R. Foster and H. C. Lukaski. Whole-body impedance—what does it measure? *The American Journal of Clinical Nutrition*, 64(3):388S–396S, 1996.
- [50] A. Guimerà, E. Calderón, P. Los, and A. M. Christie. Method and device for bio-impedance measurement with hard-tissue applications. *Physiological Measurement*, 29(6):S279, 2008.
- [51] S. F. Khalil, M. S. Mohktar, and F. Ibrahim. The theory and fundamentals of bioimpedance analysis in clinical status monitoring and diagnosis of diseases. *Sensors*, 14(6):10895–10928, 2014.
- [52] F. Simini and P. Bertemes-Filho, editors. *Bioimpedance in Biomedical Applications and Research*. Springer, 2018.
- [53] L. B. Houtkooper, T. G. Lohman, S. B. Going, and W. H. Howell. Why bioelectrical impedance analysis should be used for estimating adiposity. *The American Journal of Clinical Nutrition*, 64(3):436S–448S, 1996.
- [54] *Bioelectrical Impedance Analysis in Body Composition Measurement*. NIH Technol Assess Statement, 1994 Dec 12–14; 1–35.
- [55] P. Deurenberg, K. Van Der Kooy, R. Leenen, J. A. Weststrate, and J. C. Seidell. Sex and age specific prediction formulas for estimating body composition from bioelectrical impedance: A cross-validation study. *International Journal of Obesity*, 15(1):17–25, 1991.
- [56] H. Ogawa, K. Fujitani, T. Tsujinaka, K. Imanishi, H. Shirakata, A. Kantani, M. Hirao, Y. Kurokawa, and S. Utsumi. InBody 720 as a new method of evaluating visceral obesity. *Hepatology*, 58(105):42–44, 2011.
- [57] D-H. Lee, K. S. Park, S. Ahn, E. J. Ku, K. Y. Jung, Y. J. Kim, K. M. Kim, J. H. Moon, S. H. Choi, K. S. Park, H. C. Jang, and S. Lim. Comparison of abdominal visceral adipose tissue area measured by computed tomography with that estimated by bioelectrical impedance analysis method in korean subjects. *Nutrients*, 7(12):10513–10524, 2015.

- [58] K. S. Park, D-H. Lee, J. Lee, Y. J. Kim, K. Y. Jung, K. M. Kim, S. H. Kwak, S. H. Choi, K. S. Park, H. C. Jang, and S. Lim. Comparison between two methods of bioelectrical impedance analyses for accuracy in measuring abdominal visceral fat area. *Journal of Diabetes and Its Complications*, 30(2):343–349, 2016.
- [59] D. Berker, S. Koparal, S. Işık, L. Paşaoğlu, Y. Aydin, K. Erol, T. Delibaşı, and S. Güler. Compatibility of different methods for the measurement of visceral fat in different body mass index strata. *Diagnostic and Interventional Radiology*, 16(2):99–105, 2010.
- [60] K. H. Pietiläinen, S. Kaye, A. Karmi, L. Suojanen, A. Rissanen, and K. A. Virtanen. Agreement of bioelectrical impedance with dual-energy X-ray absorptiometry and MRI to estimate changes in body fat, skeletal muscle and visceral fat during a 12-month weight loss intervention. *British Journal of Nutrition*, 109(10):1910–1916, 2013.
- [61] InBody Co., Ltd. Inbody Technology [Online]. Retrieved from <http://www.inbody.com/global/intro/Technology.aspx>. Accessed: 1 July 2018.
- [62] InBody Co., Ltd. Report: Validation of InBody720 [Online]. Retrieved from https://www.bodyanalyse.no/studier/FFM_720vsDEXA.pdf. Accessed: 1 July 2018.
- [63] L. C. Ward. Segmental bioelectrical impedance analysis: an update. *Current Opinion in Clinical Nutrition and Metabolic Care*, 15(5):424–429, 2012.
- [64] M. Ryo, K. Maeda, T. Onda, M. Katashima, A. Okumiya, M. Nishida, T. Yamaguchi, T. Funahashi, Y. Matsuzawa, T. Nakamura, and I. Shimomura. A new simple method for the measurement of visceral fat accumulation by bioelectrical impedance. *Diabetes Care*, 28(2):451–453, 2005.
- [65] M. Nagai, H. Komiya, Y. Mori, T. Ohta, Y. Kasahara, and Y. Ikeda. Development of a new method for estimating visceral fat area with multi-frequency bioelectrical impedance. *The Tohoku Journal of Experimental Medicine*, 214(2):105–112, 2008.
- [66] J. Gómez-Ambrosi, I. González-Crespo, V. Catalán, A. Rodríguez, R. Moncada, V. Valentí, S. Romero, B. Ramírez, C. Silva, M. J. Gil, J. Salvador, A. Benito, I. Colina, and G. Frühbeck. Clinical usefulness of abdominal bioimpedance (ViScan) in the determination of visceral fat and its application in the diagnosis and management of obesity and its comorbidities. *Clinical Nutrition*, 37(2):580–589, 2018.
- [67] E. L. Thomas, A. L. Collins, J. McCarthy, J. Fitzpatrick, G. Durighel, A. P. Goldstone, and J. D. Bell. Estimation of abdominal fat compartments by bioelectrical impedance: the validity of the ViScan measurement system in comparison with MRI. *European Journal of Clinical Nutrition*, 64:525–533, 2010.
- [68] L. M. Browning, O. Mugridge, M. Chatfield, A. Dixon, S. Aitken, I. Joubert, A. M. Prentice, and S. A. Jebb. Validity of a new abdominal bioelectrical impedance device to measure abdominal and visceral fat: comparison with MRI. *Obesity (Silver Spring)*, 18(12):2385–2391, 2010.
- [69] H. Zamrazilová, P. Hlavatý, L. Dusátková, B. Sedláčková, I. A. Hainerová, M. Kunesová, A. Skoch, M. Hájek, and V. Hainer. A new simple method for estimating trunk and visceral fat by bioelectrical impedance: comparison with magnetic resonance imaging and dual x-ray absorptiometry in Czech adolescents. *Casopis Lekarů Ceskych*, 149(9):417–422, 2010.
- [70] T. Yamaguchi, K. Maki, and M. Katashima. Practical human abdominal fat imaging utilizing electrical impedance tomography. *Physiological Measurement*, 31(7):963–978, 2010.
- [71] T. F. Yamaguchi, M. Katashima, L-Q. Wang, and S. Kuriki. Improvement of image reconstruction of human abdominal conductivity by impedance tomography considering the bioelectrical anisotropy. *Advanced Biomedical Engineering*, 1:98–106, 2012.

References

- [72] T. F. Yamaguchi and Y. Okamoto. Computational method for estimating boundary of abdominal subcutaneous fat for absolute electrical impedance tomography. *International Journal for Numerical Methods in Biomedical Engineering*, 34(1):e2909, 2018.
- [73] G. G. Harrison and T. B. Van Itallie. Estimation of body composition: a new approach based on electromagnetic principles. *The American Journal of Clinical Nutrition*, 35(5):1176–1179, 1982.
- [74] E. Presta, J. Wang, G. G. Harrison, P. Björntorp, W. H. Harker, and T. B. Van Itallie. Measurement of total body electrical conductivity: a new method for estimation of body composition. *The American Journal of Clinical Nutrition*, 37(5):735–739, 1983.
- [75] A. F. Roche, S. Heymsfield, and T. G. Lohman. *Human Body Composition*. Human Kinetics, 1996.
- [76] K. Y. Lain, M. J. Garabedian, A. Daftary, and A. Jeyabalan. Neonatal adiposity following maternal treatment of gestational diabetes with glyburide compared with insulin. *American Journal of Obstetrics & Gynecology*, 200(5):501.e1–501.e6, 2009.
- [77] P. J. Chadwick and N. H. Saunders. TRIM: An electromagnetic body composition analyser. In S. Yasumura, J. E. Harrison, K. G. McNeill, A. D. Woodhead, and F. A. Dilmanian, editors, *In Vivo Body Composition Studies*, pages 387–390. Springer US, Boston, MA, 1990.
- [78] J. F. Sutcliffe, S. W. Smye, and M. A. Smith. An investigation of an electromagnetic method for the measurement of body composition. *Physics in Medicine & Biology*, 39(9):1501–1507, 1994.
- [79] J. F. Sutcliffe, S. W. Smye, and M. A. Smith. A further assessment of an electromagnetic method to measure body composition. *Physics in Medicine & Biology*, 40(4):659–670, 1995.
- [80] H. Griffiths. Magnetic induction tomography. *Measurement Science and Technology*, 12(8):1126, 2001.
- [81] H. Scharfetter, H. K. Lackner, and J. Rosell. Magnetic induction tomography: hardware for multi-frequency measurements in biological tissues. *Physiological Measurement*, 22(1):131–146, 2001.
- [82] J. R. Feldkamp. Single-coil magnetic induction tomographic three-dimensional imaging. *Journal of Medical Imaging*, 2(1):013502, 2015.
- [83] D. Gürsoy and H. Scharfetter. Feasibility of lung imaging using magnetic induction tomography. In Olaf Dössel and Wolfgang C. Schlegel, editors, *World Congress on Medical Physics and Biomedical Engineering, September 7–12, 2009, Munich, Germany*, pages 525–528, Berlin, Heidelberg, 2009. Springer Berlin Heidelberg.
- [84] J. Peltonen. A novel method for the measurement of visceral adipose tissue. Master's thesis, Helsinki University of Technology, HUT, Faculty of Electronics, Communications and Automation, Espoo, 2009. 66 pages. In Finnish.
- [85] C. Furse, D. A. Christensen, and C. H. Durney. *Basic Introduction Bioelectromagnetics, Second Edition*. CRC Press, 2009.
- [86] Selecting current sensors and transformers (General Application Note No. 1288-1). Retrieved from Coilcraft website: https://www.coilcraft.com/pdfs/Doc1288_Current_sensor_selection.pdf. Accessed: 9 Sep 2018.
- [87] K. M. Ropella. *Introduction to Statistics for Biomedical Engineers*. Morgan & Claypool Publishers, 2007.

- [88] H. Scharfetter, T. Schlager, R. Stollberger, R. Felsberger, H. Hutten, and H. Hinghofer-Szalkay. Assessing abdominal fatness with local bioimpedance analysis: basics and experimental findings. *International Journal of Obesity*, 25:502–511, 2001.
- [89] S. Watson, H. L. Blundell, W. D. Evans, H. Griffiths, R. G. Newcombe, and D. A. Rees. Can abdominal bioelectrical impedance refine the determination of visceral fat from waist circumference? *Physiological Measurement*, 30(7):N53, 2009.
- [90] D. E. Laaksonen, J. Nuutinen, T. Lahtinen, A. Rissanen, and L. K. Niskanen. Changes in abdominal subcutaneous fat water content with rapid weight loss and long-term weight maintenance in abdominally obese men and women. *International Journal of Obesity*, 27:677–683, 2003.

References

Corrigenda to Publications

Publication I, page 3, line 31

It is not correct to say that because of the skin-effect phenomenon, the eddy currents are more concentrated on the outer radius of the sample. Instead, in cylindrical sample the induced eddy currents are stronger on the outer radius of the sample, because $E_{\text{int}} = \omega Br/2$ gets stronger with the larger radius r . Skin effect, in turn, deals with how electric current flows near the outer surface of a solid electrical conductor, such as a metal wire.

Publication I, page 5, Eq. 5

The voltage change in the output voltage of the voltage divider, produced by the change in loss resistance, can be written in simpler form as

$$\Delta V \approx -\frac{V_0}{4} \frac{\Delta R_{\text{loss}}}{R_{\text{loss}}} = -\frac{V_0}{4} \frac{Q}{\omega L} \Delta R_{\text{loss}}.$$

Although being simpler, the above equation is also more accurate approximation of

$$\Delta V = \frac{V_0}{2} \frac{\Delta Z}{2Z + \Delta Z},$$

where Z is the impedance of the unloaded coil (also equal to load and source impedances of the voltage divider) and ΔZ is the change in the coil impedance when loaded. However, the improvement in accuracy has only minor effect to the reported range of observed loss resistance (page 11, line 20). With the new equation the range is 0.4–5.7 m Ω instead of 0.4–5.6 m Ω .

Publication II, page 4, Eq. 2

$m_{\text{loss,max}}$ and $m_{\text{loss,min}}$, which were not defined, are given by

$$m_{\text{loss,max}} = \frac{\bar{v}_H + \sigma_H - (\bar{v}_L - \sigma_L)}{f_H - f_L}$$
$$m_{\text{loss,min}} = \frac{\bar{v}_H - \sigma_H - (\bar{v}_L + \sigma_L)}{f_H - f_L},$$

where \bar{v}_H and \bar{v}_L are the mean values of the measured voltage changes at f_H and f_L , respectively.

Publication III, page 4, Fig. 2

The direction of the time varying magnetic field \mathbf{B} should be into the paper instead of out of the paper. Furthermore, it would be more correct to say that it is the magnitude of dB/dt , that is directed into the paper. After this correction the direction of the eddy currents shown in the Figure oppose the applied field \mathbf{B} , as it should be.

Publication V, page 200, Fig. 2

OP should be OPA, so that OP140 becomes OPA140, and OP137 becomes OPA137.



ISBN 978-952-60-8359-9 (printed)
ISBN 978-952-60-8360-5 (pdf)
ISSN 1799-4934 (printed)
ISSN 1799-4942 (pdf)

Aalto University
School of Electrical Engineering
Department of Electrical Engineering and Automation
www.aalto.fi

**BUSINESS +
ECONOMY**

**ART +
DESIGN +
ARCHITECTURE**

**SCIENCE +
TECHNOLOGY**

CROSSOVER

**DOCTORAL
DISSERTATIONS**